Unfolding a Bykov Attractor: From an Attracting Torus to Strange Attractors

Alexandre A. P. Rodrigues[1] ⬤

Abstract

In this paper we present a comprehensive mechanism for the emergence of strange attractors in a two-parametric family of differential equations acting on a three-dimensional sphere. When both parameters are zero, its flow exhibits an attracting heteroclinic network (Bykov network) made by two 1-dimensional connections and one 2-dimensional separatrix between two hyperbolic saddles-foci with different Morse indices. After slightly increasing both parameters, while keeping the one-dimensional connections unaltered, we focus our attention in the case where the two-dimensional invariant manifolds of the equilibria do not intersect. Under some conditions on the parameters and on the eigenvalues of the linearisation of the vector field at the saddle-foci, we prove the existence of many complicated dynamical objects, ranging from an attracting quasi-periodic torus to Hénon-like strange attractors, as a consequence of the *Torus-Breakdown* Theory. The mechanism for the creation of horseshoes and strange attractors is also discussed. Theoretical results are applied to show the occurrence of strange attractors in some analytic unfoldings of a Hopf-zero singularity.

Keywords Bykov attractor · Heteroclinic cycle · Torus-breakdown · Strange attractors · Hopf-zero singularity

Mathematics Subject Classification 34C28 · 34C37 · 37D05 · 37D45 · 37G35

✉ Alexandre A. P. Rodrigues
   alexandre.rodrigues@fc.up.pt

1 Centro de Matemática da Univ. do Porto, Rua do Campo Alegre, 687, 4169-007 Porto, Portugal

1 Introduction

1.1 Strange Attractors

Many aspects contribute to the richness and complexity of a dynamical system. One of them is the existence of strange attractors. Before going further, we introduce the following notion (adapted to the situation under consideration):

Definition 1 A (Hénon type) *strange attractor* of a two-dimensional dissipative diffeomorphism R defined in a Riemannian manifold, is a compact invariant set Λ with the following properties:

- Λ equals the closure of the unstable manifold of a hyperbolic periodic point;
- the basin of attraction of Λ contains an open set (and thus has positive Lebesgue measure);
- there is a dense orbit in Λ with a positive Lyapounov exponent (exponential growth of the derivative along its orbit);
- Λ is not hyperbolic.

A vector field possesses a strange attractor if the first return map to a cross section does.

The rigorous proof of the strange character of an invariant set is a great challenge and the proof of the persistence (in measure) of such attractors is a very involving task. Based on [12], Mora and Viana [37] proved the emergence of strange attractors in the process of creation or destruction of the Smale horseshoes that appear through a bifurcation of a tangential homoclinic point. In the present paper, rather than exhibit the existence of strange attractors, we explore a mechanism to guarantee the existence of such complex dynamics in the unfolding of a Bykov attractor, an expected phenomenon close to a $\mathbb{SO}(2)$-equivariant system. In the present paper, the abundance of strange attractors is a consequence of the *Torus-breakdown Theory* developed in [1,3,4,8]. See also [51].

1.2 The Object of Study

Our starting point is a two-parametric differential equation $\dot{x} = f_{(A,\lambda)}(x)$ defined in the three-dimensional sphere $\mathbb{S}^3$ with two saddle-foci sharing all the invariant manifolds of dimensions one and two for $A = \lambda = 0$, forming an attracting heteroclinic network Γ with a non-empty basin of attraction $\mathcal{U}$. We study the global transition of the dynamics from $\dot{x} = f_{(0,0)}(x)$ to a smooth two-parameter family $\dot{x} = f_{(A,\lambda)}(x)$ that breaks the network (or part of it). Note that, for small perturbations, the set $\mathcal{U}$ is still positively invariant. When $A, \lambda \neq 0$, we assume that the one-dimensional connections persist, and the two dimensional invariant manifolds are generically transverse (either intersecting or not).

When $\lambda > A \geq 0$, the two-dimensional invariant manifolds meet transversely, giving rise to a complex network, that consists of a union of Bykov cycles [17]. The dynamics in the maximal invariant set contained in $\mathcal{U}$, contains, but does not coincide with, the suspension of horseshoes accumulating on the heteroclinic network described in [6,30,33,43,44]. In addition, close to the organising center, the flow contains infinitely many heteroclinic tangencies and attracting limit cycles with long periods, coexisting with sets with positive entropy, giving rise the so called *quasi-stochastic attractors*. All dynamical models with quasi-stochastic attractors were found, either analytically or by computer simulations, to have tangencies of invariant manifolds [24].

Recently, there has been a renewal of interest of this type of heteroclinic bifurcation in the reversible [21,30,36], equivariant [33,43,44] and conservative [13] contexts.

The novelty The case $A > \lambda \geq 0$ corresponds to the situation where the two-dimensional invariant manifolds do not intersect, which has not been yet studied. Although the network Γ associated to the equilibria is destroyed, complex dynamics appears near the ghost of it. In the present article, it is shown that the perturbed system may manifest regular behavior corresponding to the existence of a smooth invariant torus, and may also have chaotic regimes. In the region of transition from regular behavior (attracting torus) to chaotic dynamics (suspended horseshoes), using known results about *Arnold tongues*, we prove the existence of lines with homoclinic tangencies to dissipative periodic solutions, responsible for the existence of persistent strange attractors nearby. This phenomenon has already been observed by [50,51] in the context of non-autonomous differential equations. Our theoretical results may be applied in specific unfoldings of the Hopf-zero singularity (Case III of [25]).

1.3 This Article

We study the dynamics arising near a differential equation with a specific attracting heteroclinic network (Bykov attractor). We show that, when a two-dimensional connection is broken with a prescribed configuration, the dynamics undergoes a global transition from regular to chaotic dynamics.

We discuss the global bifurcations that occur as the parameters (A, λ) vary. We complete our results by reducing our problem to that of a first return map having an attracting (non-contractible) curve and we study its generic bifurcations. As we will see in Sect. 9, the mechanism of the transition from regular dynamics to chaotic dynamics is not so standard as in [41,53], where just saddle-node, periodic doubling and Newhouse bifurcations were involved in the the annihilation of hyperbolic horseshoes.

This article is organised as follows. In Sect. 2, after some basic definitions, we describe precisely our object of study and in Sect. 3 we review some literature related to it. In Sect. 4 we state the main results of the article. The coordinates and other notation used in the rest of the article are presented in Sect. 5. In Sects. 6–8, we prove the main results of the manuscript. In Sect. 9, we describe generic ways to break an attracting two-dimensional torus, which involve homoclinic tangencies produced by the stable and unstable manifolds of a dissipative saddle. These tangencies are the origin of persistent strange attractors. This mechanism is discussed in Sect. 10 for generic unfoldings of the Hopf-zero singularity (Case III of [25]). For the reader's convenience, we have compiled at the end of the paper a list of definitions in a short glossary.

Throughout this paper, we have endeavoured to make a self contained exposition bringing together all topics related to the proofs. We have stated short lemmas and we have drawn illustrative figures to make the paper easily readable.

2 Setting

We will enumerate the main assumptions concerning the configuration of the network and the intersection of the invariant manifolds of the equilibria. We refer the reader to Appendix A for precise definitions.

Fig. 1 Sketch of the Bykov attractor Γ satisfying **(P1)–(P4)**
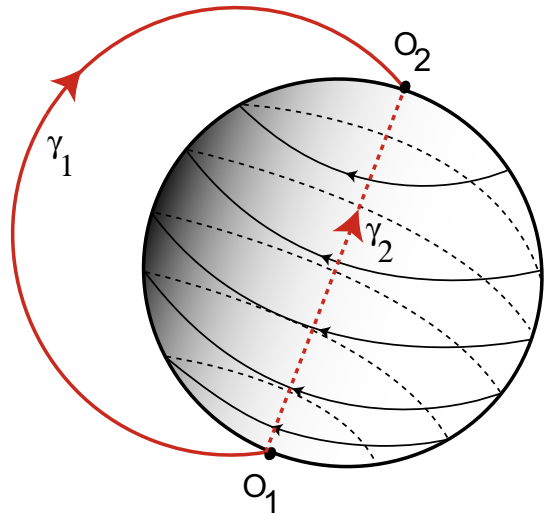
2.1 The Organising Center

For $\varepsilon > 0$ small, consider the two-parameter family of C^3-smooth differential equations

$$\dot{x} = f_{(A,\lambda)}(x) \qquad x \in \mathbb{S}^3 \qquad A, \lambda \in [0, \varepsilon] \tag{2.1}$$

where $\mathbb{S}^3$ denotes the unit three-sphere, endowed with the usual topology. Denote by $\varphi_{(A,\lambda)}(t, x), t \in \mathbb{R}$, the associated flow,[1] satisfying the following hypotheses for $A = \lambda = 0$:

(P1) There are two different equilibria, say O_1 and O_2.

(P2) The spectrum of df_x is:

    (P2a) E_1 and $-C_1 \pm \omega_1 i$ where $C_1 > E_1 > 0$, $\omega_1 > 0$,   for $x = O_1$;
    (P2b) $-C_2$ and $E_2 \pm \omega_2 i$ where $C_2 > E_2 > 0$, $\omega_2 > 0$,   for $x = O_2$.

Thus the equilibrium O_1 possesses a 2-dimensional stable and 1-dimensional unstable manifold and the equilibrium O_2 possesses a 1-dimensional stable and 2-dimensional unstable manifold. For $M \subset \mathbb{S}^3$, denoting by $\overline{M}$ the topological closure of M, we also assume that:

(P3) The manifolds $\overline{W^u(O_2)}$ and $\overline{W^s(O_1)}$ coincide and $\overline{W^u(O_2) \cap W^s(O_1)}$ consists of a two-sphere (also called the 2D-connection).

and

    (P4) There are two trajectories, say γ_1, γ_2, contained in $W^u(O_1) \cap W^s(O_2)$, one in each connected component of $\mathbb{S}^3 \backslash \overline{W^u(O_2)}$ (also called the 1D-connections).

The two equilibria O_1 and O_2, the two-dimensional heteroclinic connection from O_2 to O_1 referred in **(P3)** and the two trajectories listed in **(P4)** build a heteroclinic network we will denote hereafter by Γ. This network has two cycles and is illustrated in Fig. 1. This set has an *attracting* character [34], this is why it will be called a *Bykov attractor*.[2]

---

[1] Since $\mathbb{S}^3$ is a compact set without boundary, the local solutions of (2.1) could be extended to $\mathbb{R}$.

[2] The terminology *Bykov* is a tribute to V. Bykov who has dedicated his latest research activity to heteroclinic cycles with similar properties to those of Γ.

Fig. 2 Illustration of Property
(P5): the saddle-foci O_1 and O_2
have the same chirality
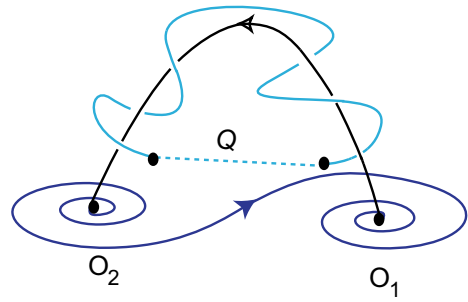
Lemma 2.1 [34] *The set Γ is asymptotically stable.*

Therefore, we may find an open neighborhood $\mathcal{U}$ of the heteroclinic network Γ having its boundary transverse to the flow of $\dot{x} = f_{(0,0)}(x)$ and such that every solution starting in $\mathcal{U}$ remains in it for all positive time and is forward asymptotic to Γ.

2.2 Chirality

There are two different possibilities for the geometry of the flow around Γ, depending on the direction in which trajectories turn around the one-dimensional heteroclinic connection from O_1 to O_2. To make this rigorous, we need some new concepts.

Let V_1 and V_2 be small disjoint neighborhoods of O_1 and O_2 with disjoint boundaries ∂V_1 and ∂V_2, respectively. These neighborhoods will be constructed with detail in Sect. 5. Trajectories starting at $\partial V_1 \setminus W^s(O_1)$ near $W^s(O_1)$ go into the interior of V_1 in positive time, then follow the connection from O_1 to O_2, go inside V_2, and then come out at ∂V_2 as in Fig. 2. Let $\mathcal{Q}$ be a piece of trajectory like the one which has been constructed from ∂V_1 to ∂V_2. Now join its starting point to its end point by a line segment as in Fig. 2, forming a closed curve, that we call the *loop* of $\mathcal{Q}$. The loop of $\mathcal{Q}$ and the network Γ are disjoint closed sets.

Definition 2 [34] We say that the two saddle-foci O_1 and O_2 in Γ have the *same chirality* if the loop of every trajectory (starting near O_1) is linked to Γ in the sense that the two closed sets cannot be disconnected by an isotopy. Otherwise, we say that O_1 and O_2 have *different chirality*.

Our next assumption is topological and may be written as:

(P5) The saddle-foci O_1 and O_2 have the same chirality.

For $r \geq 3$, denote by $\mathfrak{X}^r(\mathbb{S}^3)$, the set of C^r two-parameter families of vector fields on $\mathbb{S}^3$ satisfying Properties **(P1)–(P5)**, endowed with the C^r-topology.

2.3 Perturbing Terms

With respect to the effect of the two parameters A and λ on the dynamics, we assume that:

(P6) For $A > \lambda \geq 0$, the two trajectories within $W^u(O_1) \cap W^s(O_2)$ persist.

By Kupka-Smale Theorem, generically the invariant two-dimensional manifolds $W^u(O_2)$ and $W^s(O_1)$ are transverse (intersecting or not). Throughout this article, we assume that:

(P7a) For $A > \lambda \geq 0$, the two-dimensional manifolds $W^u(O_2)$ and $W^s(O_1)$ do not intersect.

and

(P8) The transitions along the connections $[O_1 \rightarrow O_2]$ and $[O_2 \rightarrow O_1]$ are given, in local coordinates, by the *Identity map* and by

$$(x, y) \mapsto (x, y + A + \lambda \Phi(x))$$

respectively, where $\Phi : \mathbb{S}^1 \rightarrow \mathbb{S}^1$ is a Morse function with at least two non-degenerate critical points ($\mathbb{S}^1 = \mathbb{R} \pmod{2\pi}$). This assumption will be detailed later in Sect. 5.

For the moment, without loss of generality, let us also assume that $\Phi(x) = \sin x$, $x \in \mathbb{S}^1$, which has exactly two critical points.

2.4 Constants

For future use, we settle the following notation:

$$\delta_1 = \frac{C_1}{E_1} > 1, \qquad \delta_2 = \frac{C_2}{E_2} > 1, \qquad \delta = \delta_1 \delta_2 > 1 \tag{2.2}$$

and

$$K = \frac{E_2 + C_1}{E_1 E_2} > 0, \qquad K_\omega = \frac{E_2 \omega_1 + C_1 \omega_2}{E_1 E_2} > 0 \quad \text{and} \quad a = \frac{\lambda}{A}. \tag{2.3}$$

3 Overview

In this section, we review some known results about the bifurcation of codimension 2 under consideration, which are summarized in Table 1 and illustrated in Fig. 3.

3.1 Case 1: $A = \lambda = 0$

The network Γ is asymptotically stable (see Lemma 2.1). The two-dimensional manifolds $W^u(O_2)$ and $W^s(O_1)$ coincide and the global attractor of $f_{(0,0)}$ is made of the equilibria O_1, O_2, and the two trajectories of $[O_1 \rightarrow O_2]$ together with a sphere which is both the stable manifold of O_1 and the unstable manifold of O_2. See Fig. 1.

This attractor, the so called *Bykov attractor*, has a finite number of moduli of stability and the points of its proper basin of attraction have historic behavior [18]. The coincidence of the two-dimensional invariant manifolds of O_1 and O_2 prevents visits to both cycles.

3.2 Case 2: $A = 0$ and $\lambda > 0$

Let $f_{(A,\lambda)} \in \mathfrak{X}^r(\mathbb{S}^3)$ be a two-parameter family of vector fields satisfying **(P1)–(P6)** and for which Property **(P7a)** does not hold. Trajectories within $W^u(O_1) \cap W^s(O_2)$ are kept but the manifolds $W^u(O_2)$ and $W^s(O_1)$ rearrange themselves, creating either transversal or tangential intersections. This upheaval causes an explosion of the non-wandering set of the flow, bringing forth a countable union of suspended horseshoes inside the set of trajectories that remain for all positive times in $\mathcal{U}$. These horseshoes accumulate at the stable/unstable

Table 1 Overview of the results

Case(s)	Parameters	$\lambda = 0$	$\lambda > 0$
1 and 2	$A = 0$	Attracting network [33,35]	Horseshoes + strange attractors [35] + homoclinic tangencies [35,45]
3	$0 < A < \lambda$	–	Horseshoes + strange attractors [35] + homoclinic tangencies [35,45]
4 (new)	$A > \lambda$	Attracting torus	Torus or horseshoes + strange attractors (additional parameter: K_ω)
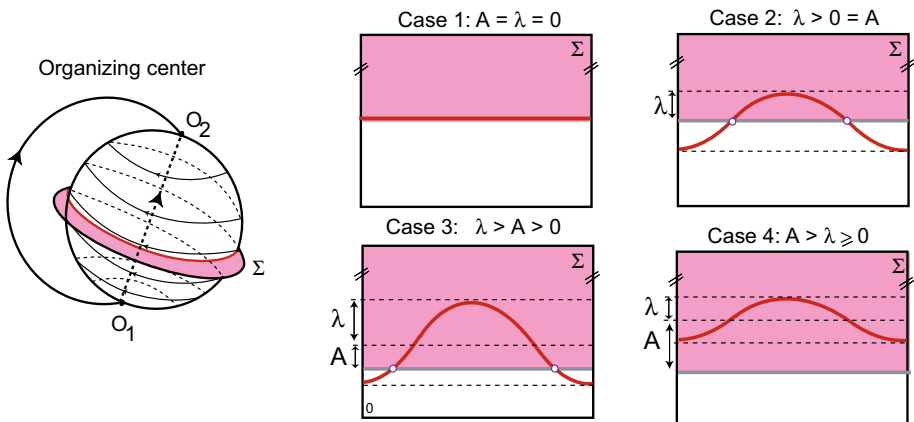
Fig. 3 Shape of the first hit of $W^u(O_2)/W^s(O_1)$ to Σ. The set Σ a cross section to the Bykov attractor Γ near the connection $W^u(O_2) \cap W^s(O_1)$. The symbol $\circ$ represents (transverse) heteroclinic connections from O_2 to O_1; the red line is the graph of $\Phi(x)$ representing $W^u(O_2) \cap \Sigma$; the grey line is $W^s(O_1) \cap \Sigma$; the double bars mean that the sides are identified (Color figure online)

manifolds of the equilibria (cf. [17,33]). Furthermore, for a sequence of positive parameters arbitrarily close to zero, say $(\lambda_j)_j$, the flow associated to $f_{(0,\lambda_j)}$ exhibits homo and heteroclinic tangencies, sinks with long periods and strange attractors (cf. [35,37,38]).

3.3 Case 3: $\lambda > A > 0$

In this case, the manifolds $W^u(O_2)$ and $W^s(O_1)$ still meet transversely along at least two connections and thus the results of [33,35,44] still hold. The transverse intersection of the two-dimensional invariant manifolds of the two equilibria implies that the set of trajectories that remain for all time in a small neighborhood of the Bykov cycle contains a locally-maximal hyperbolic set admitting a complete description in terms of symbolic dynamics, reminiscent of the results of [24,47]. An obstacle to the global symbolic description of these trajectories is the existence of tangencies that lead to the birth of stable periodic solutions, as described in [23,24,39].

3.4 Case 4: $A > \lambda \geq 0$

As far as we know, the cases $A > \lambda = 0$ and $A > \lambda > 0$ have not been studied. The goal of this article is to explore these cases where there are no cycles associated to O_1 and O_2. In contrast to Cases 2 and 3, where the involved bifurcations are related to horseshoe destruction, tangencies and Newhouse phenomena [35,41], in Case 4 the bifurcations are connected with the *Torus-Breakdown Theory* [1,3,4,8]. Hence, hereafter, we also assume that:

   (P7b) $A > \lambda \geq 0$ (or, equivalently, $a = \frac{\lambda}{A} \in [\, 0, 1\, [\,)$.

   Under hypothesis **(P8)**, one has **(P7a)** $\Leftrightarrow$ **(P7b)**, as noticed in Remark 5.2. When we refer to **(P7)** we refer one of the above.

   For $r \geq 3$, we denote by $\mathfrak{X}^r_{\text{Byk}}(\mathbb{S}^3) \subset \mathfrak{X}^r(\mathbb{S}^3)$, the set of C^r two-parameter families of vector fields on $\mathbb{S}^3$ satisfying conditions **(P1)–(P8)**. An explicit example with a two parameter polynomial differential equation satisfying **(P1)–(P7)** has been given in §4.1.3.2 of [5].

Digestive remark

Constants A and λ may be interpreted as follows: as depicted in Fig. 3, the first hit of $W^u(O_2)$ and $W^s(O_1)$ to Σ are two closed curves. In Case 4, according to our model, the distance between the two curves can be written as $A + \lambda \Phi(x)$, $x \in \mathbb{S}^1$, which may be seen as an approximation of the Melnikov function associated to the two-dimensional invariant manifolds [25, §4.5]. The constant A gives the averaged distance between the first hit of $W^u(O_2)$ and $W^s(O_1)$ in Σ; the parameter λ describes fluctuations of $W^u(O_2)$ in Σ.

4 Main Results

Let $\mathcal{T}$ be a neighborhood of the Bykov attractor Γ, which exists for $A = \lambda = 0$. For $\varepsilon > 0$ small, let $\big(f_{(A,\lambda)}\big)_{(A,\lambda)\in[0,\varepsilon]^2}$ be a two-parameter family of vector fields in $\mathfrak{X}^3_{Byk}(\mathbb{S}^3)$ satisfying conditions **(P1)–(P8)**.

Theorem A *Let $f_{(A,\lambda)} \in \mathfrak{X}^3_{Byk}(\mathbb{S}^3)$. Then, there is $\tilde{\varepsilon} > 0$ (small) such that the first return map to a given cross section to Γ may be written (in local coordinates) by:*

$$\mathcal{F}_{(A,\lambda)}(x, y) = \big[x - K_\omega \ln(y + A + \lambda \sin x) \quad (\text{mod } 2\pi), \quad (y + A + \lambda \sin x)^\delta\big] + \cdots$$

where

$$(x, y) \in \mathcal{D} = \{x \in \mathbb{R} \quad (\text{mod } 2\pi), \quad y/\tilde{\varepsilon} \in [-1, 1] \;\; and \;\; y + A + \lambda \sin x > 0\}$$

and the ellipsis stand for asymptotically small terms depending on x and y which converge to zero along their derivatives.

   The proof of Theorem A is done in Sect. 6 by composing local and transition maps. Since $\delta > 1$, for A small enough, the second component of $\mathcal{F}_{(A,\lambda)}$ is contracting and, under an additional hypothesis, the dynamics of $\mathcal{F}_{(A,\lambda)}$ is dominated by the family of circle maps.

Theorem B *Let $f_{(A,\lambda)} \in \mathfrak{X}^3_{Byk}(\mathbb{S}^3)$. For $A > 0$ small enough, if $\frac{\lambda}{A} < \frac{1}{\sqrt{1+K_\omega^2}}$, then there is an invariant closed curve $\mathcal{C} \subset \mathcal{D}$ as the maximal attractor for $\mathcal{F}_{(A,\lambda)}$. This closed curve is not contractible on $\mathcal{D}$.*
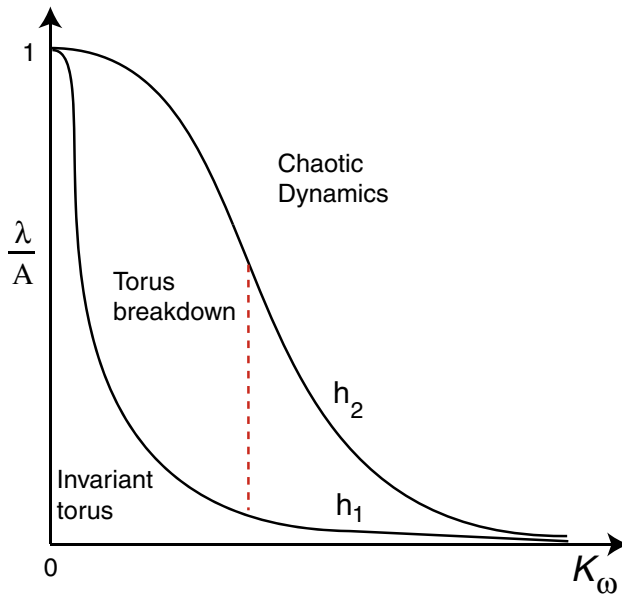
Fig. 4 Invariant attracting 2-torus and chaotic regions for the map $\mathcal{F}_{(A,\lambda)}$ with respect to the parameters K_ω and $\frac{\lambda}{A}$

The proof of Theorem is performed in Sect. 7 using the Afraimovich's Annulus Principle [3]. The curve $\mathcal{C}$ is *globally attracting* in the sense that, for every $p \in \mathcal{D}$, there exist a point $p_0 \in \mathcal{C}$ such that

$$\lim_{n \to +\infty} \left| \mathcal{F}_{(A,\lambda)}^n(p) - \mathcal{F}_{(A,\lambda)}^n(p_0) \right| = 0.$$

The attracting invariant curve for $\mathcal{F}_{(A,\lambda)}$ is the graph of a smooth map and corresponds to an attracting two-torus for the flow of (2.1). Thus, in particular:

Corollary C *Let* $f_{(A,\lambda)} \in \mathfrak{X}_{Byk}^3(\mathbb{S}^3)$. *For* $A > 0$ *small enough, if either* $K_\omega > 0$ *or* $\lambda > 0$ *are sufficiently small, then:*

(a) *there is a persistent two-dimensional torus which is globally attracting.*
(b) *the dynamics of* $\mathcal{F}_{(A,\lambda)}$ *induces on* $\mathcal{C}$ *a circle map. In this case, for any given interval of unit length I, there is a positive measure set* $\Delta \subset I$ *so that the rotation number of* $\mathcal{F}_{(A,\lambda)}|_\mathcal{C}$ *is irrational if and only if* $a = \lambda/A \in \Delta$.

Proof (a) The existence of an invariant torus is a direct corollary of Theorem B. Since the torus is normally hyperbolic, its persistence follows from the theory for normally hyperbolic manifolds developed by Hirsch et al. [27].

(b) The first part of this item follows from (a); the second part, concerning the rotation number on circle maps, may be found in Boyland [15] and Herman [26].   □

The previous result implies the existence of a set of positive Lebesgue measure (in the bifurcation parameter (A, λ)) for which the torus has a dense orbit, i.e. the whole torus is a minimal attractor.

Theorem D *Let* $f_{(A,\lambda)} \in \mathfrak{X}^3_{Byk}(\mathbb{S}^3)$. *For* $A > 0$ *small enough, if*

$$\frac{\exp\left(\frac{6\pi}{K_\omega}\right) - 1}{\exp\left(\frac{6\pi}{K_\omega}\right) - 1/6} < \frac{\lambda}{A} < 1,$$

then there exists a hyperbolic invariant closed subset Λ *in a cross section to* Γ *such that* $\mathcal{F}_{(A,\lambda)}|_\Lambda$ *is topologically conjugate to the Bernoulli shift of two symbols.*

Remark 4.1 Under a stronger hypothesis, the conclusion of Theorem D may be rephrased as: $\mathcal{F}_{(A,\lambda)}|_\Lambda$ is topologically conjugate to the Bernoulli shift of m symbols, with $2 \leq m \in \mathbb{N}$, giving rise to *rotational horseshoes*, a particular type of horseshoes characterized by Passegi et al. [42]—see Lemma 8.2.

As a corollary of Theorems B and D, in the bifurcation diagram $(a, K_\omega) = \left(\frac{\lambda}{A}, K_\omega\right)$, we may draw, in the first quadrant, two smooth curves, the graphs of h_1 and h_2 in Fig. 4, such that:

(1) $h_1(K_\omega) = \frac{1}{\sqrt{1+K_\omega^2}}$ and $f(K_\omega) = \frac{\exp\left(\frac{6\pi}{K_\omega}\right)-1}{\exp\left(\frac{6\pi}{K_\omega}\right)-1/6}$;

(2) the region below the graph of h_1 corresponds to flows having an invariant and attracting torus with zero topological entropy (regular dynamics);

(3) the region above the graph of h_2 corresponds to vector fields whose flows exhibit suspended horseshoes (chaotic dynamics).

The behavior of $\mathcal{F}_{(A,\lambda)}$ is unknown for the parameter range between the graphs of f and g. Nevertheless, for $K_\omega > 0$ fixed (along the red dashed line in Fig. 4), the transition from the graph of h_1 to that of h_2 may be explained *via* Arnold tongues associated to the torus bifurcations [1,7,8]. In particular, in the bifurcation diagram $\left(A, \frac{\lambda}{A}\right)$, there is a set with positive Lebesgue measure for which the family (2.1) exhibits strange attractors.

Theorem E *Fix* $K_\omega^0 > 0$. *In the bifurcation diagram* $\left(A, \frac{\lambda}{A}\right)$, *where* (A, λ) *is such that* $h_1(K_\omega^0) < \frac{\lambda}{A} < h_2(K_\omega^0)$, *there exists a positive measure set* Δ *of parameter values, so that for every* $a \in \Delta$, $\mathcal{F}_{(A,\lambda)}$ *admits a strange attractor (of Hénon-type) with an ergodic SRB measure.*

The proof of Theorem E is a consequence of the *Torus-Breakdown Theory* [1,3,4,8] combined with the results by Mora and Viana [37]. A discussion of these results will be performed in Sect. 9.

An Application: Strange Attractors in the Unfolding of a Hopf-Zero Singularity

By applying the previous theory, we may show the occurrence of strange attractors in a specific case of unfoldings of a Hopf-zero singularity (Type I of [11], Case III of [25]).[3] Since the hypotheses are very technical, we decide to postpone the precise result to Sect. 10.

---

[3] Care is needed to compare both works because the constants choice and signs are different.
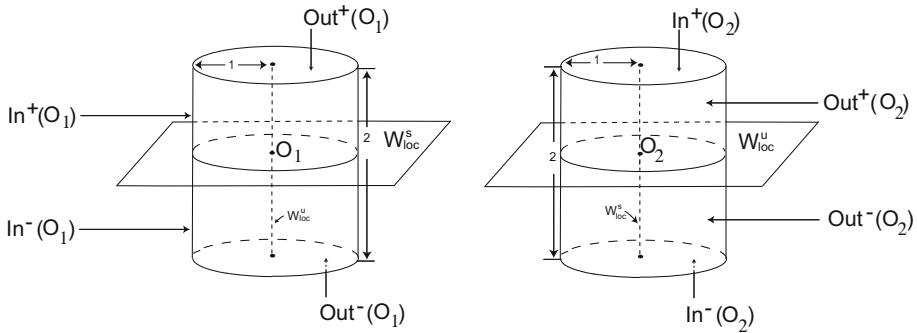
Fig. 5 Local cylindrical coordinates inside V_1 and V_2 and near O_1 and O_2, respectively

5 Local and Transition Maps

In this section we will analyze the dynamics near the Bykov attractor Γ through local maps, after selecting appropriate coordinates in neighborhoods of the saddle-foci O_1 and O_2 (see Fig. 5), as done in [40].

5.1 Local Coordinates

In order to describe the dynamics around the cycles of Γ, we use the local coordinates near the equilibria O_1 and O_2 introduced in [35]. See also Ovsyannikov and Shilnikov [40].

In these coordinates, we consider cylindrical neighborhoods V_1 and V_2 in $\mathbb{R}^3$ of O_1 and O_2, respectively, of radius $\rho = \tilde{\varepsilon} > 0$ and height $z = 2\tilde{\varepsilon}$—see Fig. 5. After a linear rescaling of the variables, we may also assume that $\tilde{\varepsilon} = 1$. Their boundaries consist of three components: the cylinder wall parametrised by $x \in \mathbb{R}$ (mod 2π) and $|y| \leq 1$ with the usual cover

$$(x, y) \mapsto (1, x, y) = (\rho, \theta, z)$$

and two discs, the top and bottom of the cylinder. We take polar coverings of these disks

$$(r, \varphi) \mapsto (r, \varphi, \pm 1) = (\rho, \theta, z)$$

where $0 \leq r \leq 1$ and $\varphi \in \mathbb{R}$ (mod 2π). The local stable manifold of O_1, $W_{\mathrm{loc}}^s(O_1)$, corresponds to the circle parametrised by $y = 0$. In V_1 we use the following terminology suggested in Fig. 5:

- In(O_1), the cylinder wall of V_1, consisting of points that go inside V_1 in positive time;
- Out(O_1), the top and bottom of V_1, consisting of points that go outside V_1 in positive time.

We denote by $\mathrm{In}^+(O_1)$ the upper part of the cylinder, parametrised by (x, y), $y \in\,]0, 1]$ and by $\mathrm{In}^-(O_1)$ its lower part.

The cross-sections obtained for the linearisation around O_2 are dual to these. The set $W_{\mathrm{loc}}^s(O_2)$ is the z-axis intersecting the top and bottom of the cylinder V_2 at the origin of its coordinates. The set $W_{\mathrm{loc}}^u(O_2)$ is parametrised by $y = 0$, and we use:

- In(O_2), the top and bottom of V_2, consisting of points that go inside V_2 in positive time;

- Out(O_2), the cylinder wall of V_2, consisting of points that go inside V_2 in negative time, with Out$^+(O_2)$ denoting its upper part, parametrised by (x, y), $y \in]0, 1]$ and Out$^-(O_2)$ its lower part.

We will denote by $W^u_{\text{loc}}(O_2)$ the portion of $W^u(O_2)$ that goes from O_2 up to In(O_1) not intersecting the interior of V_1 and by $W^s_{\text{loc}}(O_1)$ the portion of $W^s(O_1)$ outside V_2 that goes directly from Out(O_2) into O_1. The flow is transverse to these cross-sections and the boundaries of V_1 and of V_2 may be written as the closure of In$(O_1) \cup$ Out(O_1) and In$(O_2) \cup$ Out(O_2), respectively. The orientation of the angular coordinate near O_2 is chosen to be compatible with the direction induced by the angular coordinate in O_1.

5.2 Local Maps Near the Saddle-Foci

Following [20,40], the trajectory of a point (x, y) with $y > 0$ in In$^+(O_1)$, leaves V_1 at Out(O_1) at

$$\Phi_1(x, y) = \left(y^{\delta_1} + S_1(x, y; A, \lambda), -\frac{\omega_1 \ln y}{E_1} + x + S_2(x, y; A, \lambda) \right)$$

$$= (r, \phi) \quad \text{where} \quad \delta_1 = \frac{C_1}{E_1} > 1, \tag{5.1}$$

where S_1, S_2 are smooth functions which depend on A, λ and satisfy:

$$\left| \frac{\partial^{k+l+m_1+m_2}}{\partial x^k \partial y^l \partial \lambda^{m_1} \partial A^{m_2}} S_i(x, y; A, \lambda) \right| \leq C \, y^{\delta_1 + \sigma - l}. \tag{5.2}$$

The numbers C, σ are positive constants and k, l, m_1, m_2 are non-negative integers. Similarly, a point (r, ϕ) in In$(O_2) \backslash W^s_{\text{loc}}(O_2)$, leaves V_2 at Out(O_2) at

$$\Phi_2(r, \varphi) = \left(-\frac{\omega_2 \ln r}{E_2} + \varphi + R_1(r, \varphi; A, \lambda), r^{\delta_2} + R_2(r, \varphi; A, \lambda) \right) = (x, y)$$

$$\text{where} \quad \delta_2 = \frac{C_2}{E_2} > 1 \tag{5.3}$$

and R_1, R_2 satisfy a condition similar to (5.2). The terms S_1, S_2, R_1, R_2 correspond to asymptotically small terms that vanish when y and r go to zero. A better estimate under a stronger eigenvalue condition has been obtained in [28, Prop. 2.4].

5.3 The Transitions

The coordinates on V_1 and V_2 are chosen so that $[O_1 \to O_2]$ connects points with $z > 0$ (resp. $z < 0$) in V_1 to points with $z > 0$ (resp. $z < 0$) in V_2. Points in Out$(O_1) \setminus W^u_{\text{loc}}(O_1)$ near $W^u(O_1)$ are mapped into In(O_2) along a flow-box around each of the connections $[O_1 \to O_2]$. Assuming **(P8)**, the transition

$$\Psi_{1\to2}: \quad \text{Out}(O_1) \quad \to \quad \text{In}(O_2)$$

does not depend neither on λ nor A and is the Identity map, a choice compatible with Hypothesis **(P4)**. Using a more general form for $\Psi_{1\to2}$ would complicate the computations without any change in the final results. Denote by η the map

$$\eta = \Phi_2 \circ \Psi_{1\to2} \circ \Phi_1: \quad \text{In}(O_1) \quad \to \quad \text{Out}(O_2).$$
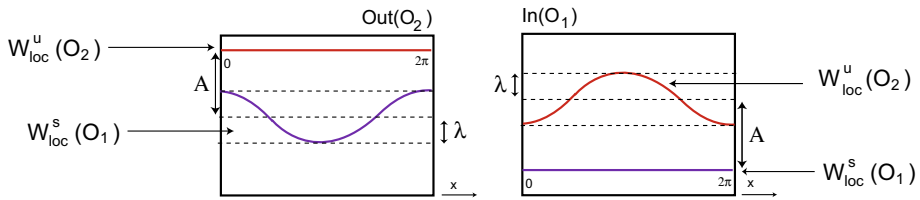
Fig. 6 Geometry of the global map $\Psi_{2\to1}^{(A,\lambda)}$. For $A > \lambda \geq 0$, $W_{loc}^{s}(O_1)$ intersects the wall $Out(O_2)$ of the cylinder V_2 and $W_{loc}^{u}(O_2)$ intersects the wall $In(O_1)$ of the cylinder V_1 on closed curves given, in local coordinates, by the graph of a 2π−periodic function of sinusoidal type. Compare with Figure 4 of [22]

Omitting the higher order terms which appear in (5.1) and (5.3), we infer that, in local coordinates, for $y > 0$ we have

$$\eta(x, y) = \left(x - K_\omega \ln y \mod 2\pi, \ y^\delta\right) \tag{5.4}$$

with

$$\delta = \delta_1 \delta_2 > 1 \quad \text{and} \quad K_\omega = \frac{C_1 \omega_2 + E_2 \omega_1}{E_1 E_2} > 0. \tag{5.5}$$

A similar expression is valid for $y < 0$, after suitable changes in the sign of y. Using **(P7)** and **(P8)**, for $A > \lambda \geq 0$, we still have a well defined transition map

$$\Psi_{2\to1}^{(A,\lambda)} : Out(O_2) \to In(O_1)$$

that depends on the parameters λ and A, given by (see Fig. 6)

$$\Psi_{2\to1}^{(A,\lambda)}(x, y) = (x, \ y + A + \lambda \sin x). \tag{5.6}$$

Remark 5.1 Our study is based on a model satisfying Hypothesis **(P8)**. It governs the transition maps along the heteroclinic connections, being necessary to make precise computations in Sects. 6–8. The part concerning the transition along $[O_2 \to O_1]$, $\Psi_{2\to1}^{(A,\lambda)}$, corresponds to the expected unfolding from the coincidence of the two-dimensional invariant manifolds at $f_{(0,0)}$; this is also suggested in Figure 4 of [22].

Remark 5.2 We are now in conditions to explain why, under **(P8)**, the hypotheses **(P7a)** and **(P7b)** are equivalent. Indeed, as suggested by Fig. 6, the sets $W_{loc}^{u}(O_2) \cap Out(O_2)$ and $W_{loc}^{s}(O_1) \cap In(O_1)$ are parametrised by $y = 0$. Assuming **(P8)**, the set

$$\Psi_{2\to1}^{(A,\lambda)}(W_{loc}^{u}(O_2) \cap Out(O_2)) \subset In(O_1)$$

is the graph of $A + \lambda \sin(x), x \in \mathbb{S}^1$. Since $A, \lambda \geq 0$, the two-dimensional manifolds $W_{loc}^{u}(O_2)$ and $W_{loc}^{s}(O_1)$ do not intersect if and only if

$$A + \lambda \sin(x) > 0, \qquad x \in \mathbb{S}^1.$$

In particular, $A > \lambda \geq 0$ i.e. $\lambda/A \in [0, 1[$.

To simplify the notation, in what follows we will sometimes drop the subscript (A, λ), unless there is some risk of misunderstanding.

6 Proof of Theorem A

The proof of Theorem A is straightforward by composing the local and transition maps constructed in Sect. 5. Let

$$\mathcal{F}_{(A,\lambda)} = \eta \circ \Psi_{2 \to 1} =: \quad \mathcal{D} \subset \text{Out}(O_2) \quad \to \quad \mathcal{D} \subset \text{Out}(O_2). \tag{6.1}$$

be the first return map to $\text{Out}(O_2)$, where $\mathcal{D}$ is the set of initial conditions $(x, y) \in \text{Out}(O_2)$ whose solution returns to $\text{Out}(O_2)$. Composing η (5.4) with $\Psi_{2\to 1}$ (5.6), the analytic expression of $\mathcal{F}_{(A,\lambda)}$ is given by:

$$\mathcal{F}_{(A,\lambda)}(x, y) = \left[-K_\omega \ln \left[y + A + \lambda \sin x \right] + x \quad (\text{mod } 2\pi), \; (y + A + \lambda \sin x)^\delta \right]$$

$$= \left(\mathcal{F}_1^{(A,\lambda)}(x, y), \mathcal{F}_2^{(A,\lambda)}(x, y) \right),$$

and Theorem A is proved.

The following technical result will be useful in the sequel.

Lemma 6.1 *For $A > 0$ small enough, the map $\mathcal{F}_2^{(A,\lambda)}$ is a contraction in the variable y.*

Proof Since $\delta > 1$ and $y \in [0, 1]$, we may write:

$$\left| \frac{\partial \mathcal{F}_2^{(A,\lambda)}(x, y)}{\partial y} \right| = \left| \delta (y + A + \lambda \sin x)^{\delta - 1} \right| = O(A^{\delta - 1}) < 1,$$

and we get the result. $\qquad\qquad\qquad\qquad\qquad\qquad\qquad\qquad\qquad\qquad\qquad\qquad\qquad\qquad\qquad$ □

7 Proof of Theorem B

To prove the existence of an invariant and attracting smooth closed curve for $\mathcal{F}_{(A,\lambda)}$, we make use if the *Afraimovich Annulus Principle* [3,4]. We start by proving the existence of a flow-invariant annulus in $\text{Out}^+(O_2)$ in Sect. 7.1, then we check the conditions required by the Annulus Principle (one by one) in Sect. 7.2.

7.1 The Existence of an Annulus

Let

$$\mathcal{B} = \left\{ (x, y) : A^\delta \left(1 - \frac{\lambda}{A} \right)^\delta \leq y \leq 2A^\delta \left(1 + \frac{\lambda}{A} \right)^\delta \quad \text{and} \quad x \in \mathbb{R} \quad (\text{mod } 2\pi) \right\} \subset \text{Out}^+(O_2)$$

In what follows, if $\mathcal{X} \subset \text{Out}(O_2)$, let $\overset{\circ}{\mathcal{X}}$ denote the topological interior of $\mathcal{X}$.

Lemma 7.1 *There exists $A_0 \in]0, \varepsilon[$ such that: if $A \in]0, A_0]$ and $\lambda \in [0, A[$ then $\mathcal{F}_{(A,\lambda)}(\mathcal{B}) \subseteq \overset{\circ}{\mathcal{B}}$.*

Proof If $(x, y) \in \mathcal{B}$, we have:

$$(y + A + \lambda \sin x)^\delta = A^\delta \left(\frac{y}{A} + 1 + \frac{\lambda}{A} \sin x \right)^\delta$$

$$\leq A^\delta \left(2A^{\delta-1} \left(1 + \frac{\lambda}{A} \right)^\delta + 1 + \frac{\lambda}{A} \right)^\delta + o(1) \, y^\delta$$

$$\leq A^\delta \left(\left(1 + \frac{\lambda}{A} \right) \left(2A^{\delta-1} \left(1 + \frac{\lambda}{A} \right)^{\delta-1} + 1 \right) \right)^\delta$$

$$\leq A^\delta \left(1 + \frac{\lambda}{A} \right)^\delta \left(O\left(A^\delta \right) + 1 \right)$$

$$< 2A^\delta \left(1 + \frac{\lambda}{A} \right)^\delta,$$

In particular, there exists $A_1 > 0$ such that:

$$\forall A < A_1, \ \forall \lambda < A, \qquad (y + A + \lambda \sin x)^\delta < 2A^\delta \left(1 + \frac{\lambda}{A} \right)^\delta.$$

Analogously, if $(x, y) \in \mathcal{B}$, we may write:

$$(y + A + \lambda \sin x)^\delta = A^\delta \left(\frac{y}{A} + 1 + \frac{\lambda}{A} \sin x \right)^\delta$$

$$\geq A^\delta \left(A^{\delta-1} \left(1 - \frac{\lambda}{A} \right)^\delta + 1 - \frac{\lambda}{A} \right)^\delta$$

$$\geq A^\delta \left(\left(1 - \frac{\lambda}{A} \right) \left(A^{\delta-1} \left(1 - \frac{\lambda}{A} \right)^{\delta-1} + 1 \right) \right)^\delta$$

$$\geq A^\delta \left(1 - \frac{\lambda}{A} \right)^\delta \left(O\left(A^\delta \right) + 1 \right)^\delta$$

$$> A^\delta \left(1 - \frac{\lambda}{A} \right)^\delta$$

Therefore, there exists $A_2 > 0$ such that:

$$\forall A < A_2, \ \forall \lambda < A \qquad (y + A + \lambda \sin x)^\delta > A^\delta \left(1 - \frac{\lambda}{A} \right)^\delta.$$

Therefore, the region $\mathcal{B}$ is forward invariant for all $A \in \,]0, A_0]$ and $\lambda \in [0, A[$, where $A_0 = \min\{A_1, A_2\}$. $\qquad\square$

We recall the annulus principle (version [4]), adapted to our purposes. Let us introduce the following notation: for a vector-valued or matrix-valued function $\mathbf{F}(x, y)$, define

$$\|\mathbf{F}\| = \sup_{(x,y) \in \mathcal{B}} \|\mathbf{F}(x, y)\|,$$

where $\|\star\|$ is the standard Euclidian norm.

Theorem 7.2 [4] *Let* $G(x, y) = (x + g_1(x, y), g_2(x, y))$ *be a* C^1 *map, with* $x \in \mathbb{R}$ (mod 2π), *defined on the annulus*

$$\mathcal{B} = \{(x, y) : a \leq y \leq b \text{ and } x \in \mathbb{R} \pmod{2\pi}\},$$

where $0 < a < b$, and satisfying:

(1) g_1 and g_2 are 2π-periodic in x and smooth;

(2) $G(\mathcal{B}) \subseteq \overset{\circ}{\mathcal{B}}$;

(3) $0 < \left\| 1 + \dfrac{\partial g_1}{\partial x} \right\| < 1$;

(4) $\left\| \dfrac{\partial g_2}{\partial y} \right\| < 1$ (ie, the map g_2 is a contraction in y);

(5) $2\sqrt{\left\| 1 + \dfrac{\partial g_1}{\partial x} \right\|^{-2} \left\| \dfrac{\partial g_2}{\partial x} \right\| \left\| \dfrac{\partial g_1}{\partial y} \right\|} < 1 - \left\| 1 + \dfrac{\partial g_1}{\partial x} \right\|^{-1} \left\| \dfrac{\partial g_2}{\partial y} \right\|$;

(6) $\left\| 1 + \dfrac{\partial g_1}{\partial x} \right\| + \left\| \dfrac{\partial g_2}{\partial y} \right\| < 2$,

then the maximal attractor in $\mathcal{B}$ is an invariant closed curve, the graph of a 2π-periodic, C^1 function $y = h(x)$.

7.2 Proof of Theorem B

In this section, we prove Theorem B as an application of Theorem 7.2. Let us define:

$$g_1(x, y) = \mathcal{F}_1^{(A,\lambda)}(x, y) - x = -K_\omega \ln(y + A + \lambda \sin x)$$

$$g_2(x, y) = \mathcal{F}_2^{(A,\lambda)}(x, y) = (y + A + \lambda \sin x)^\delta$$

where

$$K_\omega = \frac{C_1 \omega_2 + E_2 \omega_1}{E_1 E_2},$$

whose derivatives may be written as:

$$\frac{\partial g_1(x, y)}{\partial x} = -K_\omega \frac{\lambda \cos x}{y + A + \lambda \sin x},$$

$$\frac{\partial g_1(x, y)}{\partial y} = \frac{-K_\omega}{y + A + \lambda \sin x},$$

$$\frac{\partial g_2(x, y)}{\partial x} = \delta\lambda(y + A + \lambda \sin x)^{\delta-1} \cos x,$$

$$\frac{\partial g_2(x, y)}{\partial y} = \delta(y + A + \lambda \sin x)^{\delta-1}.$$

We state and prove an auxiliary result that will be used in the sequel.

Lemma 7.3 *If $0 < \lambda < \dfrac{A}{\sqrt{1+K_\omega^2}}$, the range of $\dfrac{\partial \mathcal{F}_1^{(A,\lambda)}}{\partial x}$ is $]0, 1[$.*

Proof First note that

$$\frac{\partial \mathcal{F}_1^{(A,\lambda)}}{\partial x} = 1 + \frac{\partial g_1(x, y)}{\partial x} = 1 - K_\omega \frac{\frac{\lambda}{A} \cos x}{1 + \frac{\lambda}{A} \sin x} + o(1) y. \tag{7.1}$$

Taking $a = \frac{\lambda}{A}$, we get:

$$\frac{\partial^2 \mathcal{F}_1^{(A,\lambda)}}{\partial^2 x} = \frac{\partial \left(1 + \frac{\partial g_1(x,y)}{\partial x} \right)}{\partial x} = \frac{\partial}{\partial x} \left(1 - K_\omega \frac{a \cos x}{1 + a \sin x} \right)$$

$$= K_\omega \frac{a \sin x (1 + a \sin(x)) + a^2 \cos^2(x)}{(1 + a \sin(x))^2}$$

$$= K_\omega \frac{a \sin x + a^2}{(1 + a \sin(x))^2}$$

Therefore $\frac{\partial^2 \mathcal{F}_1^{(A,\lambda)}(x,y)}{\partial^2 x} = 0$ if and only if $a = 0$ or $\sin(x) = -a$. Let us define $x^\star \in [\pi, 3\pi/2]$ such that $\sin(x^\star) = -a$. Therefore:

$$0 < 1 + \frac{\partial g_1(x^\star, y)}{\partial x} < 1 \Leftrightarrow 0 < 1 - K_\omega \frac{a \cos x^\star}{1 + a \sin x^\star} < 1$$

$$\Leftrightarrow 0 < 1 - \frac{K_\omega a \sqrt{1 - a^2}}{1 - a^2} < 1$$

$$\Leftrightarrow 0 < \frac{K_\omega a}{\sqrt{1 - a^2}} < 1$$

$$\Leftrightarrow \frac{1 - a^2}{a^2} > K_\omega^2$$

$$\Leftrightarrow a < \frac{1}{\sqrt{K_\omega^2 + 1}}$$

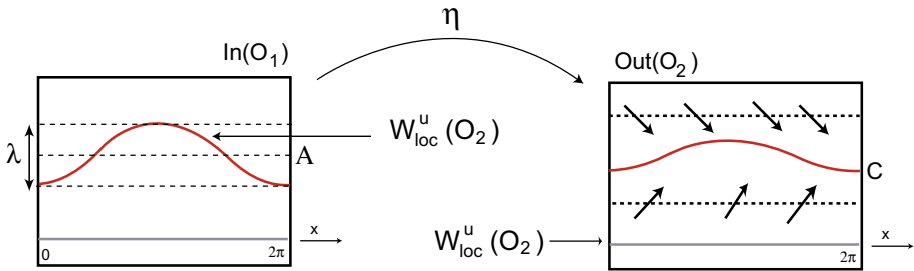$$\Leftrightarrow \lambda < \frac{A}{\sqrt{K_\omega^2 + 1}}$$

$\square$

In order to prove Theorem B, we check one by one the hypotheses of Theorem 7.2, putting all pieces together.

(1) It is easy to see to see that $g_1(x, y) = \mathcal{F}_1^{(A,\lambda)}(x, y) - x$ and $g_2(x, y) = \mathcal{F}_2^{(A,\lambda)}(x, y)$ are 2π-periodic in the variable x and smooth in $\mathcal{B}$.

(2) This item follows from Lemma 7.1, where $a = A^\delta \left(1 - \frac{\lambda}{A}\right)^\delta$ and $b = 2A^\delta \left(1 + \frac{\lambda}{A}\right)^\delta$.

(3) Using Lemma 7.3, we know that $0 < \left\| 1 + \frac{\partial g_1}{\partial x} \right\| < 1$ if $a = \frac{\lambda}{A} \in [0, \frac{1}{\sqrt{1+K_\omega^2}}[$. In particular, under the same condition, we get $\left\| 1 + \frac{\partial g_1}{\partial x} \right\|^{-1} < \infty$.

(4) The proof of this item follows from Lemma 6.1. Indeed,

$$\left\| \frac{\partial g_2(x, y)}{\partial y} \right\| = \sup_{(x,y) \in \mathcal{B}} |\delta(y + A + \lambda \sin x)^{\delta-1}| = O(A^{\delta-1}) < 1.$$

(5) Since

$$\frac{\partial g_1(x, y)}{\partial y} = \frac{-K_\omega}{y + A + \lambda \sin x} = O\left(\frac{1}{A}\right) \quad \text{and}$$

$$\frac{\partial g_2(x, y)}{\partial x} = \delta\lambda(y + A + \lambda \sin x)^{\delta-1} \cos x$$

$$\leq \delta A(y + A + \lambda \sin x)^{\delta-1}$$

$$= O\left(A^\delta\right),$$

Fig. 7 Illustration of Theorem B: for $A > 0$ small enough, if $\lambda < \frac{A}{\sqrt{1+K_\omega^2}}$, then there is an invariant closed curve $\mathcal{C} \subset \text{Out}^+(O_2)$ as the maximal attractor of $\mathcal{F}_{(A,\lambda)}$

this implies that:

$$\sqrt{\left\|1 + \frac{\partial g_1}{\partial x}\right\|^{-2} \left\|\frac{\partial g_2}{\partial x}\right\| \left\|\frac{\partial g_1}{\partial y}\right\|} = \left\|1 + \frac{\partial g_1}{\partial x}\right\|^{-1} O(A^{\delta/2}) \, O(A^{-1/2}) = O\left(A^{\frac{\delta-1}{2}}\right).$$

Combining now

$$1 - \left\|1 + \frac{\partial g_1}{\partial x}\right\|^{-1} \left\|\frac{\partial g_2}{\partial y}\right\| = 1 - O\left(A^{\delta-1}\right)$$

with

$$\sqrt{\left\|1 + \frac{\partial g_1}{\partial x}\right\|^{-2} \left\|\frac{\partial g_2}{\partial x}\right\| \left\|\frac{\partial g_1}{\partial y}\right\|} = O\left(A^{\frac{\delta-1}{2}}\right),$$

item (5) follows for $A > 0$ sufficiently small.

(6) Using again Lemmas 6.1 and 7.3, we get:

$$\left\|1 + \frac{\partial g_1}{\partial x}\right\| + \left\|\frac{\partial g_2}{\partial y}\right\| < 1 + O(A^{\delta-1}) < 2$$

This ends the proof of the existence of an attracting curve for the dynamics of $\mathcal{F}_{(A,\lambda)}$, provided $A > 0$ is sufficiently small and $\frac{\lambda}{A} < \frac{1}{\sqrt{1+K_\omega^2}}$. This curve, shown is Fig. 7, is not contractible because it is the graph of a C^1-smooth map h.

Geometric Interpretation

Condition $\lambda < \frac{A}{\sqrt{1+K_\omega^2}}$ implies that the image of the annulus $\mathcal{B}$ under $\mathcal{F}_{(A,\lambda)}$ is also an annulus bounded by two curves without folds. The subsequent image of this annulus is self-alike too, and so on. As a result, we obtain a sequence of embedded annuli; the contraction in the y-variable (Lemma 6.1) guarantees that these annuli intersect in a single and smooth attracting closed curve.

8 Proof of Theorem D

In this section, under an appropriate hypothesis, we prove the existence of two rectangles whose image under $\mathcal{F}_{(A,\lambda)}$ overlaps with $\mathrm{Out}(O_2)$ at least twice. Therefore, we obtain a construction similar to the hyperbolic Smale horseshoe: a small tubular neighborhood of $y = 0$ (in $\mathrm{Out}(O_2)$) is folded and mapped into itself.

8.1 Stretching the Angular Component

The first technical result, illustrated in Fig. 8, says that the image under $\mathcal{F}_1^{(A,\lambda)}$ of the segment parametrised by

$$\left\{ (x, y) \in \mathcal{D} : \quad \frac{\pi}{2} < x < \frac{3\pi}{2} \quad \text{and} \quad y = y_0 \right\}$$

($y_0 \in [0, 1]$) is monotonic, meaning that there are no folds. Here we use the hypothesis that the map $\Phi(x) = \sin x$ has non-degenerate critical points.

Lemma 8.1 *For any $y_0 \in [0, 1]$, the angular map $\mathcal{F}_1^{(A,\lambda)}(x, y_0)$ is an increasing map for* $x \in \,]\pi/2, 3\pi/2[$.

Proof Let $y_0 \in [0, 1]$. One knows that:

$$\frac{\partial \mathcal{F}_1^{(A,\lambda)}}{\partial x}(x, y_0) = 1 - K_\omega \frac{\lambda \cos x}{y_0 + A + \lambda \sin x}$$

$$= 1 - K_\omega \frac{\frac{\lambda}{A} \cos x}{\frac{y_0}{A} + 1 + \frac{\lambda}{A} \sin x}$$

$$\approx 1 - K_\omega \frac{\frac{\lambda}{A} \cos x}{1 + \frac{\lambda}{A} \sin x}$$

Since $\frac{\lambda}{A} \ll 1$ and $\frac{\lambda}{A} \cos x < 0$ in $\,]\pi/2, 3\pi/2[$, we may conclude that:

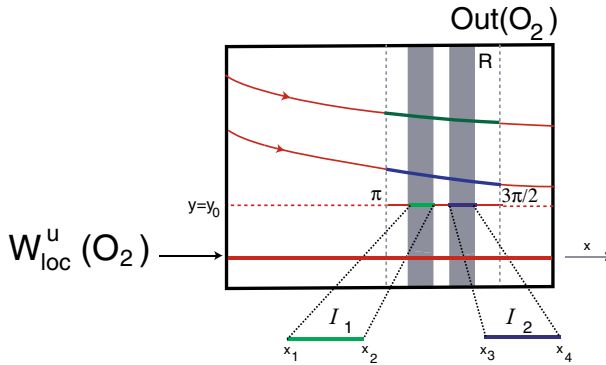$$\forall x \in \,]\pi/2, 3\pi/2[, \qquad \frac{\partial \mathcal{F}_1^{(A,\lambda)}}{\partial x}(x, y_0) > 0$$

and the result follows.   □

From now on, for $n \in \mathbb{N}\backslash\{1\}$, let $\theta_n = \pi + \arcsin(c_n)$ where $c_n = \frac{1}{2(n+1)}$. It is easy to see that $\theta_n \in \,]\pi, 3\pi/2[$ and $\sin(\theta_n) = \sin(\pi + \arcsin(c_n)) = -c_n < 0$.

Therefore, for all $y \in [0, 1]$ and $\delta \in [0, 3\pi/2 - \theta_n[\subset]0, \pi/2[$, we have:

$$\mathcal{F}_1^{(A,\lambda)}(3\pi/2 - \delta, y) - \mathcal{F}_1^{(A,\lambda)}(\theta_n, y)$$

$$= -K_\omega \ln[y + A + \lambda \sin(3\pi/2 - \delta)] + (3\pi/2 - \delta)$$
$$+ K_\omega \ln(y + A + \lambda \sin \theta_n) - \theta_n$$

$$= (3\pi/2 - \delta - \theta_n) + K_\omega \ln \left[\frac{y + A + \lambda \sin \theta_n}{y + A + \lambda \sin(3\pi/2 - \delta)} \right]$$

Fig. 8 For $y_0 \in [0, 1]$, the image under $\mathcal{F}_{(A,\lambda)}$ of the segment $[\pi, 3\pi/2] \times \{y_0\}$ is a curve (without folds) intersecting twice the rectangle $R = [\pi, 3\pi/2] \times [-1, 1] \subset \mathrm{Out}(O_2)$. There are two sub-segments (I_1 and I_2) which are stretched by $\mathcal{F}_{(A,\lambda)}$ along R

$$= (3\pi/2 - \delta - \theta_n) + K_\omega \ln \left[\frac{\frac{1}{A} y + 1 + \frac{\lambda}{A} \sin \theta_n}{\frac{1}{A} y + 1 + \frac{\lambda}{A} \sin(3\pi/2 - \delta)} \right]$$

$$= (3\pi/2 - \delta - \theta_n) + K_\omega \ln \left[\frac{1 - \frac{\lambda c_n}{A}}{1 - \frac{\lambda}{A} \cos(\delta)} \right] + o(1) \, y \tag{8.1}$$

For each $n \in \mathbb{N}\backslash\{1\}$, $\delta \in \,]0, \pi/2[$, $a = \frac{\lambda}{A} \in [0, 1[$ and $A \neq 0$, define the map

$$P(\delta, a) := K_\omega \ln \left[\frac{1 - a \, c_n}{1 - a \cos(\delta)} \right]. \tag{8.2}$$

Lemma 8.2 *For* $n \in \mathbb{N}\backslash\{1\}$, $\frac{\lambda}{A} > \dfrac{\exp\left(\frac{\pi}{K_\omega c_n}\right) - 1}{\exp\left(\frac{\pi}{K_\omega c_n}\right) - c_n}$ *if and only if* $P\left(0, \frac{\lambda}{A}\right) > \frac{\pi}{c_n}$.

Proof Taking $a = \lambda/A$, we may write:

$$P(0, a) > \frac{\pi}{c_n} \Leftrightarrow K_\omega \ln \left(\frac{1 - a \, c_n}{1 - a \cos 0} \right) > \frac{\pi}{c_n}$$

$$\Leftrightarrow \ln \left(\frac{1 - a \, c_n}{1 - a} \right) > \frac{\pi}{K_\omega \, c_n}$$

$$\Leftrightarrow \frac{1 - a \, c_n}{1 - a} > \exp \left(\frac{\pi}{K_\omega \, c_n} \right)$$

$$\Leftrightarrow 1 - a \, c_n > (1 - a) \exp \left(\frac{\pi}{K_\omega \, c_n} \right)$$

$$\Leftrightarrow 1 - a \, c_n > \exp \left(\frac{\pi}{K_\omega \, c_n} \right) - a \exp \left(\frac{\pi}{K_\omega \, c_n} \right)$$

$$\Leftrightarrow a \left(\exp \left(\frac{\pi}{K_\omega \, c_n} \right) - c_n \right) > \exp \left(\frac{\pi}{K_\omega \, c_n} \right) - 1$$

$$\Leftrightarrow a > \frac{\exp \left(\frac{\pi}{K_\omega \, c_n} \right) - 1}{\left(\exp \left(\frac{\pi}{K_\omega \, c_n} \right) - c_n \right)}$$

$\square$

Using Lemma 8.2, by continuity of P with respect to δ, there exists $\delta_0 < 3\pi/2 - \theta_n$ such that

$$\frac{\lambda}{A} > \frac{\exp\left(\frac{\pi}{K_\omega c_n}\right) - 1}{\left(\exp\left(\frac{\pi}{K_\omega c_n}\right) - c_n\right)} \quad\quad \Rightarrow \quad\quad P\left(\delta_0, \frac{\lambda}{A}\right) > \frac{\pi}{c_n} = 2(n+1)\pi. \quad\quad (8.3)$$

Taking into account (8.1), the condition $3\pi/2 - \delta - \theta_n \in [0, \pi/2]$, and (8.3), we conclude that there exists $\delta_0 < 3\pi/2 - \theta_n$ such that

$$\mathcal{F}_1^{(A,\lambda)}(3\pi/2 - \delta_0, y) - \mathcal{F}_1^{(A,\lambda)}(\theta_n, y) > 2n\pi + \frac{3\pi}{2}.$$

Then, as suggested in Fig. 8, the image, under $\mathcal{F}_{(A,\lambda)}$, of the segment $[\pi, 3\pi/2] \times \{y_0\}$ is a curve (without folds) intersecting n times the rectangle

$$R = [\pi, 3\pi/2] \times [-1, 1] \subset \mathrm{Out}(O_2).$$

In particular, we may find n disjoint intervals defined by $I_n = [x_{2n-1}, x_{2n}]$ such that

$$\pi < \theta_n < x_1 < x_2 < \cdots < x_{2n-1} < x_{2n} < \frac{3\pi}{2} - \delta_0, \quad\quad (8.4)$$

for which we define n non-empty compact and disjoint subsets H_n, on which the map $\mathcal{F}_{(A,\lambda)}|_{H_1 \cup \cdots \cup H_n}$ is topologically conjugate to a Bernoulli shift with n symbols. The construction of this horseshoe ($n = 2$) is the goal of the Sect. 8.2.

8.2 The Construction of the Topological Horseshoe

We now recall the main steps of the construction of the horseshoes (with $n = 2$) which are $\mathcal{F}_{(A,\lambda)}$–invariant. The argument uses the generalized Conley-Moser conditions [25,32, 46,52] to ensure the existence for $\frac{\lambda}{A} > \frac{\exp\left(\frac{\pi}{K_\omega c_2}\right) - 1}{\exp\left(\frac{\pi}{K_\omega c_2}\right) - c_2}$, of an invariant set $\Lambda \subset \mathrm{Out}^+(O_2)$ topologically conjugated to a Bernoulli shift with 2 symbols. As suggested in Fig. 9 (right), in this subsection, we decided to flip coordinates $(x, y) \leftrightarrow (y, x)$ in $\mathcal{D} \subset \mathrm{Out}(O_2)$ because doing so, we get a high similarity of the present situation to that of [44,52], where we address the reader for details.

Given a rectangular region $\mathcal{R}$ in $\mathrm{Out}(O_2)$, parameterised by a rectangle $[w_1, w_2] \times [z_1, z_2]$, a *horizontal strip* in $\mathcal{R}$ is a set

$$\mathcal{H} = \{(y, x) : x \in [u_1(y), u_2(y)] \quad\quad y \in [w_1, w_2]\}$$

where $u_1, u_2 : [w_1, w_2] \to [z_1, z_2]$ are Lipschitz functions such that $u_1(y) < u_2(y)$. The *horizontal boundaries* of a horizontal strip are the graphs of the maps u_i; the *vertical boundaries* are the lines $\{w_i\} \times [u_1(w_i), u_2(w_i)]$. In an analogous way, we define a *vertical strip across* $\mathrm{Out}(O_2)$, a *vertical rectangle*, with the roles of x and y reversed.
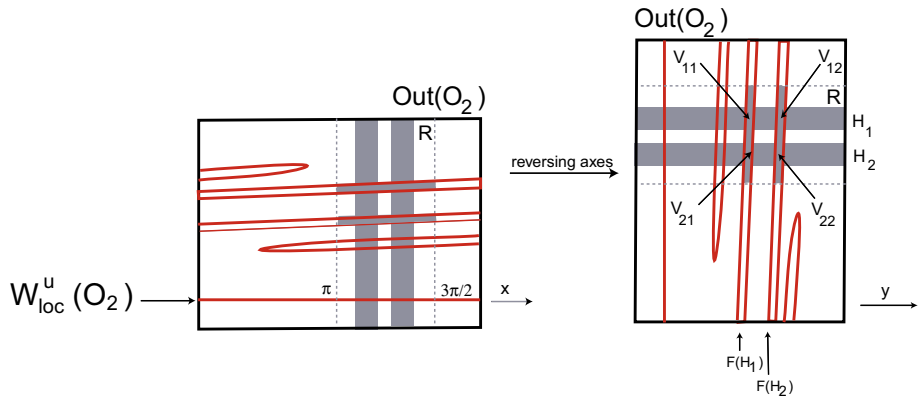
We may deduce (by construction) that:

(1) For $i = 1, 2$, as suggested in Fig. 9, the horizontal strip

$$H_i = \{(y, x) \in \mathcal{D} : x \in I_i\}.$$

is mapped (homeomorphically) by $\mathcal{F}_{(A,\lambda)}$ into a vertical strip across $R \subset \mathrm{Out}(O_2)$.

(2) $\mathcal{F}_{(A,\lambda)}(H_1) \cap \mathcal{F}_{(A,\lambda)}(H_2) = \emptyset$ because $\mathcal{F}_{(A,\lambda)}$ is a diffeomorphism, where it is well defined.

Fig. 9 Two rectangles whose image under $\mathcal{F}_{(A,\lambda)}$ overlaps with Out(O_2) at least twice, giving rise to a Smale horseshoe—see Fig. 10d

(3) $\mathcal{F}_{(A,\lambda)}(H_1)$ and $\mathcal{F}_{(A,\lambda)}(H_2)$ have full intersections with H_1 and H_2 (*i.e.* the vertical boundaries of $\mathcal{F}_{(A,\lambda)}(H_1)$ and $\mathcal{F}_{(A,\lambda)}(H_2)$ cross both the horizontal and vertical boundaries of H_1 and H_2) because of Lemma 8.2 and subsequent remark;

(4) For $i, j = 1, 2$, defining $V_{ji} := \mathcal{F}_{(A,\lambda)}(H_i) \cap H_j$, $H_{ij} := \mathcal{F}_{(A,\lambda)}^{-1}(V_{ji}) = H_i \cap \mathcal{F}_{(A,\lambda)}^{-1}(H_j)$ and denoting by $\partial_v V_{ji}$ the vertical boundaries of V_{ji}, we get, by construction, that:

    (1) $\partial_v V_{ji} \subset \partial_v \mathcal{F}_{(A,\lambda)}(H_i)$;

    (2) the map $\mathcal{F}_{(A,\lambda)}$ maps H_{ij} homomorphically onto V_{ji};

    (3) $\mathcal{F}_{(A,\lambda)}^{-1}(\partial_v V_{ji}) \subset \partial_v H_i$.

Using [52], we may conclude that there exists a $\mathcal{F}_{(A,\lambda)}$−invariant set of initial conditions

$$\Lambda = \bigcap_{n \in \mathbb{Z}} \mathcal{F}_{(A,\lambda)}^n (H_1 \cup H_2)$$

on which the map $\mathcal{F}_{(A,\lambda)}|_\Lambda$ is topologically conjugate to a Bernoulli shift with two symbols.

8.3 Hyperbolicity

To prove the hyperbolicity of Λ with respect to the map $\mathcal{F}_{(A,\lambda)}$, we apply the following result due to Afraimovich et al. [2].

Theorem 8.3 [2] *Let $H : U \to \mathbb{R}^2$ be a C^1 map where U is an open convex subset of $\mathbb{R}^2$ such that $H(x, y) := (F_1(x, y), F_2(x, y))$, where $x, y \in \mathbb{R}$. If:*

(1) $\left\| \frac{\partial F_2}{\partial y} \right\| < 1$

(2) $\left\| \left(\frac{\partial F_1}{\partial x} \right)^{-1} \right\| < 1$;

(3) $1 - \left\| \frac{\partial F_2}{\partial y} \right\| \left\| \left(\frac{\partial F_1}{\partial x} \right)^{-1} \right\| > 2 \sqrt{ \left\| \frac{\partial F_2}{\partial x} \right\| \left\| \frac{\partial F_1}{\partial y} \right\| \left\| \left(\frac{\partial F_1}{\partial x} \right)^{-1} \right\| }$

(4) $\left(1 - \left\| \frac{\partial F_2}{\partial y} \right\| \right) \left(1 - \left\| \frac{\partial F_1}{\partial x} \right\|^{-1} \right) > \left\| \frac{\partial F_2}{\partial x} \right\| \left\| (\frac{\partial F_1}{\partial x})^{-1} \right\| \left\| \frac{\partial F_1}{\partial y} \right\|$,

then any compact invariant set $\Lambda \subset U$ is hyperbolic.

To finish the proof of Theorem D, we check one by one the hypotheses of Theorem 8.3, when applied to the compact set $\Lambda \subset \mathrm{Out}^+(O_2)$, where $F_1 = \mathcal{F}_1^{(A,\lambda)}$ and $F_2 = \mathcal{F}_2^{(A,\lambda)}$.

(1) The proof follows from Lemma 6.1.
(2) One knows that:

$$\left\| \left(\frac{\partial F_1}{\partial x} \right) \right\| = \sup_{(x,y) \in \Lambda} \left| \left(\frac{\partial F_1}{\partial x} \right) \right|$$

$$= \sup_{(x,y) \in \Lambda} \left| 1 - K_\omega \frac{\frac{\lambda}{A} \cos x}{1 + \frac{\lambda}{A} \sin x} + o(1) \, y \right| > 1$$

The last inequality follows from the fact that $\pi < x < \frac{3\pi}{2}$ (see (8.4)) in $\Lambda \subset H_1 \cup H_2$.

(3) By Lemma 6.1, it follows that:

$$1 - \left\| \frac{\partial F_2}{\partial y} \right\| \left\| \left(\frac{\partial F_1}{\partial x} \right)^{-1} \right\| = 1 - O(A^{\delta-1}) \left\| \left(\frac{\partial F_1}{\partial x} \right)^{-1} \right\|$$

On the other hand, we may write:

$$2 \sqrt{ \left\| \frac{\partial F_2}{\partial x} \right\| \left\| \frac{\partial F_1}{\partial y} \right\| \left\| \left(\frac{\partial F_1}{\partial x} \right)^{-1} \right\| } = 2 \sqrt{ \left\| \left(\frac{\partial F_1}{\partial x} \right)^{-1} \right\| } \, O(A^{\frac{\delta-1}{2}})$$

(4) Similarly, we write:

$$\left(1 - \left\| \frac{\partial F_2}{\partial y} \right\| \right) \left(1 - \left\| \frac{\partial F_1}{\partial x} \right\|^{-1} \right) = (1 - O(A^\delta)) \left(1 - \left\| \frac{\partial F_1}{\partial x} \right\|^{-1} \right)$$

and

$$\left\| \frac{\partial F_2}{\partial x} \right\| \left\| \left(\frac{\partial F_1}{\partial x} \right)^{-1} \right\| \left\| \frac{\partial F_1}{\partial y} \right\| = O(A^\delta) \left\| \left(\frac{\partial F_1}{\partial x} \right)^{-1} \right\| O(A^{-1})$$

Geometric Interpretation

Condition $a = \frac{\lambda}{A} > \frac{\exp\left(\frac{\pi}{K_\omega c_2} \right) - 1}{\exp\left(\frac{\pi}{K_\omega c_2} \right) - c_2}$ provides enough expansion in the x-variable (angular coordinate) within the region $R \subset \mathrm{Out}(O_2)$. It means that there are at least two rectangles whose image under $\mathcal{F}_{(A,\lambda)}$ overlaps with $R \subset \mathrm{Out}(O_2)$ at least twice, giving rise to a suspended horseshoe. Hyperbolicity is obtained by considering rectangles whose vertical boundaries do not have reversals of orientation.

Remark 8.4 The dynamics of Λ is mainly governed by the geometric configuration of the global invariant manifold $W^u(O_2)$.

9 Proof of Theorem E

In the bifurcation diagram $\left(\frac{\lambda}{A}, K_\omega \right)$, we may draw two smooth curves in the first quadrant, the graphs of h_1 and h_2, such that:
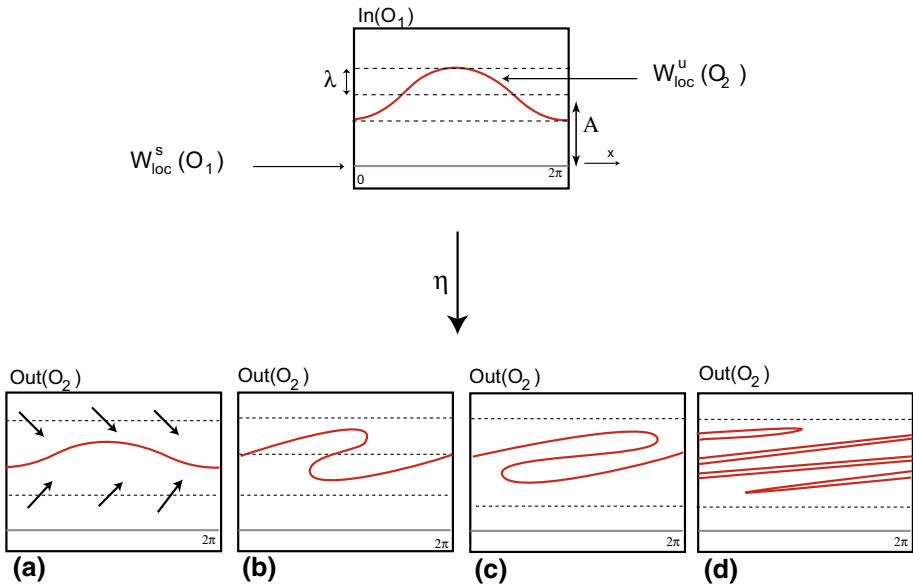
Fig. 10 Image of $\eta(W^u(O_2) \cap \text{In}(O_1))$ for different values of $\frac{\lambda}{A}$ with K_ω^0 fixed. Transition from an invariant and attracting curve (**a**) to a horseshoe (**d**) for a fixed $K_\omega^0 > 0$ and λ/A increasing. One observes the "breaking of the wave" which accompanies the break of the invariant circle $\mathcal{C}$. In **d**, a neighborhood of $y = 0$ is folded and mapped into itself, leading to the formation of horseshoes—see Fig. 9

(1) $h_1(K_\omega) = \dfrac{1}{\sqrt{1 + K_\omega^2}}$ and $h_2(K_\omega) = \dfrac{\exp\left(\frac{6\pi}{K_\omega}\right) - 1}{\exp\left(\frac{6\pi}{K_\omega}\right) - 1/6}$;

(2) the region below the graph of h_1 corresponds to flows having an invariant and attracting torus with zero topological entropy (regular dynamics);

(3) the region above the graph of h_2 corresponds to vector fields whose flows exhibit chaos (chaotic dynamics).

For A, $K_\omega > 0$ fixed, as λ increases, one observes the "breaking of the wave" which accompanies the break of the invariant circle $\mathcal{C}$. As suggested in Fig. 10, the attracting curve $\mathcal{C}$ (whose existence is ensured by Theorem B) starts to disintegrate into a finite collection of periodic saddles and sinks, a phenomenon occurring within an Arnold tongue. Once the horseshoes develop, they persist.

In what follows, we describe generic mechanisms to break an attracting two-dimensional torus which involves the onset of homoclinic tangencies produced by the stable and unstable manifolds of a dissipative saddle.[4] These tangencies are the source of strange attractors. We address the reader to [1,3,4,8] for more information on the subject. A comprehensive description of these phenomena has been given by Shilnikov et al. [48].

---

[4] Note that, for small $A, \lambda > 0$, the first return map $\mathcal{F}_{(A,\lambda)}$ is still contracting.
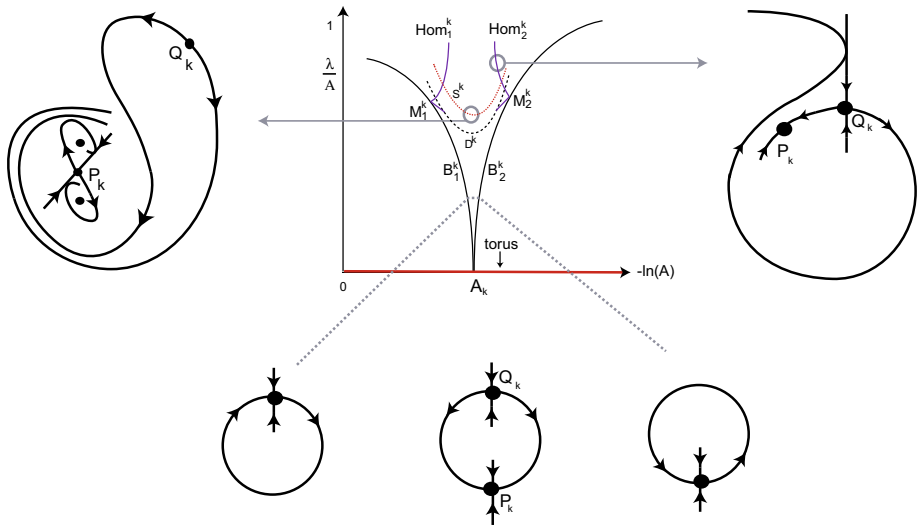
Fig. 11 In the Arnold tongue $\mathcal{T}_k$, there are three lines corresponding to the emergence of a homoclinic tangency associated to a dissipative periodic point. Left: homoclinic tangency of third class which occurs along S^k; right: homoclinic tangencies which occur along the lines Hom_1^k, Hom_2^k. Center: B_k^1 and B_k^2: saddle-node bifurcations; D^k: period doubling bifurcation (torus-breakdown); M_k^1, M_k^2: above these points, the maximal invariant set is not homeomorphic to a circle; Q_k: saddle; P_k: sink. Source: [8,48]

9.1 Dissecting an Arnold Tongue

For $\varepsilon > 0$ small, the choice of parameters in Sect. 2 ($\varepsilon > A > \lambda \geq 0$) lets us to build the bifurcation diagram of Fig. 11, in the domain

$$\{0 \leq -\ln A, \ 0 < \lambda/A < 1\} \quad \subset \quad [0, +\infty[\ \times [0, 1].$$

We suggest that the reader follows this subsection observing Fig. 11.

Within the region above, for each $k \in \mathbb{N}$, we may define an Arnold tongue (or resonance wedge), denoted by $\mathcal{T}_k$, adjoining the horizontal axis at a point $A_k = (\exp(-2\pi k), 0)$. Parameters within this wedge correspond to Poincaré maps with at least a pair of fixed points; one of the fixed points is always of saddle-type (say Q_k); the other point is a sink (say P_k). We suppose just one pair of fixed points for the following analysis (as shown in Fig. 11).

The borders of the Arnold tongue $\mathcal{T}_k$ are the bifurcation curves B_1^k and B_2^k on which the fixed points merge to a saddle-node. The curve B_2^k continue up to the line $\lambda/A = 1$, while the curve B_1^k bends to the left staying below $\lambda/A = 1$. Eventually these curves may touch the corresponding curves of other tongue, meaning that there are parameter values for which the periodic points of periods k and m coexist, $m, k \in \mathbb{N}$.

The points M_1^k and M_2^k correspond to *pre-wiggles*: below these points, in B_1^k and B_2^k, the limit set of $W^u(Q_k)$ is the saddle-node itself and is homeomorphic to a circle. Above this point, the maximal invariant set is not homeomorphic to a circle. There is also a curve, say D^k, above which the invariant torus (or the curve $\mathcal{C}$) no longer exists due to period doubling bifurcation process [7].

In the next subsection we will emphasise the role played by the lines Hom_1^k, Hom_2^k and S^k, also depicted in Fig. 11.

9.2 Strange Attractors

Continuing the process of dissecting an Arnold tongue, the authors of [1,7] describe generic mechanisms by which the invariant and attracting torus is destroyed. Two of them are revived in the next result and involve homoclinic tangencies—routes [PA] and [PB] of [7].

Theorem 9.1 ([1,7], adapted) *For $K_\omega^0 > 0$ fixed, in the bifurcation diagram $\left(-\ln A, \frac{\lambda}{A}\right)$, within $\mathcal{T}_k$:*

(1) *there are two curves Hom_1^k and Hom_2^k corresponding to a homoclinic tangency associated to a dissipative periodic point of the first return map $\mathcal{F}_{(A,\lambda)}$.*

(2) *there is one curve S^k corresponding to a homoclinic tangency (of third class) associated to a dissipative periodic point of the first return map $\mathcal{F}_{(A,\lambda)}$.*

Along the bifurcation curves Hom_1^k and Hom_2^k, one observes a homoclinic contact of the components $W^s(Q_k)$ and $W^u(Q_k)$, where Q_k is a dissipative saddle, as illustrated in Fig. 11(right). The curves Hom_1^k and Hom_2^k divide the region above D^k into two regions with simple and complex dynamics. In the zone above the curves Hom_1^k and Hom_2^k, there is a fixed point Q_k exhibiting a transverse homoclinic intersection, and thus the corresponding map $\mathcal{F}_{(A,\lambda)}$ exhibits nontrivial hyperbolic chaotic sets. Other stable points of large period exist in the region above the curves Hom_1^k and Hom_2^k since the homoclinic tangencies arising in these lines are generic [19,39]. The curve S^k corresponds to a homoclinic tangency of third class meaning that there are tangencies associated to the fixed points which have emerged from the period-doubling bifurcation at D^k (see the meaning of D^k in Sect. 9.1). Again, above these curves, in the parameter space $(-\ln A, \frac{\lambda}{A})$, there is a dense set of parameters for which the map $\mathcal{F}_{(A,\lambda)}$ has infinitely many sinks. The next result will be used to finish the proof of Theorem E:

Theorem 9.2 [37] *Let $(f_\mu)_\mu$ a one-parameter family of diffeomorphisms on a surface S and suppose that for f_{μ_0} has a homoclinic tangency associated to a dissipative periodic point $q \in S$. Then, under generic conditions, there is a positive Lebesgue measure set E of parameter values near μ_0 such that for all $\mu \in E$, the diffeomorphism f_μ exhibits a Hénon-like strange attractor near the orbit of tangency (with an ergodic SRB measure).*

By Theorem 9.1, the existence of Hom_1^k, Hom_2^k and S^k shows that there are curves in the space of parameters $\left(A, \frac{\lambda}{A}\right)$ for which the corresponding first return map has a quadratic (generic) homoclinic tangency associated to a dissipative periodic point of the first return map $\mathcal{F}_{(A,\lambda)}$. Using now Theorem 9.2, there exists a positive measure set Δ of parameter values, so that for every $a \in \Delta$, $\mathcal{F}_{(A,\lambda)}$ admits a strange attractor of Hénon-type with an ergodic SRB measure. This completes the proof of Theorem E.

Remark 9.3 In this type of result, the number of connected components with which the strange attractors intersect the section $\mathrm{Out}(O_2)$ is not specified nor is the size of their basins of attraction.

Remark 9.4 In **(P4)** we have asked for the existence of two 1D-connections. Nevertheless the statements of Theorems B, D and E still hold if **(P4)** is replaced by:

(P4a) There is one trajectory contained in $W^u(O_1) \cap W^s(O_2)$,

provided the map $\Psi_{2\rightarrow1}^{(A,\lambda)}$ sends the line $W_{\mathrm{loc}}^u(O_2) \cap \mathrm{Out}(O_2)$ into the connected component of $\mathrm{In}(O_1) \backslash W_{\mathrm{loc}}^s(O_1)$ where solutions follow the 1D-connection. This remark will be important in Sect. 10.

10 An Application: Hopf-Zero Singularity Unfolds Strange Attractors

In this section, we prove the existence of strange attractors in particular analytic unfoldings of a Hopf-zero singularity. In order to improve the readability of the paper, we recall to the reader the most important steps about unfoldings of a Hopf-zero singularity.

From now on, we consider Hopf-Zero singularities, that is, three-dimensional vector fields f^* in $\mathbb{R}^3$ such that:

- $O \equiv (0, 0, 0)$ is an equilibrium of $f^\star$;
- the spectrum of $df^*(0, 0, 0)$ is $\{\pm i\omega, 0\}$, with $\omega > 0$.

Without loss of generality, we can assume that:

$$Df^*(0, 0, 0) = \begin{bmatrix} 0 & \omega & 0 \\ -\omega & 0 & 0 \\ 0 & 0 & 0 \end{bmatrix}. \tag{10.1}$$

Observe that the lowest codimension singularities in $\mathbb{R}^3$ with a three-dimensional center manifold are the ones whose linear part is linearly conjugated to (10.1).

10.1 The Normal Form

The normal form of a degenerate jet with linear part given by $\begin{bmatrix} 0 & \omega & 0 \\ -\omega & 0 & 0 \\ 0 & 0 & 0 \end{bmatrix} \begin{bmatrix} x \\ y \\ z \end{bmatrix}$ may be written in cylindrical coordinates (r, θ, z) by:

$$\begin{cases} \dot{r} = a_1 rz + a_2 r^3 + a_3 rz^2 + O(|r, z|^4) \\ \dot{\theta} = \omega + O(|r, z|^2) \\ \dot{z} = b_1 r^2 + b_2 z^2 + b_3 r^2 z + b_4 z^3 + O(|r, z|^4) \end{cases} \tag{10.2}$$

where $\omega > 0$ and $a_1, a_2, a_3, b_1, b_2, b_3, b_4 \in \mathbb{R}\backslash\{0\}$. Normal form can be chosen in such a way that, up to arbitrarily high $k \in \mathbb{N}$, the truncation of order k contains no θ-dependent terms [25]. Ultimately, one has to restore the tail which, generically, contains no θ-dependent terms.[5] Truncating (10.2) at order 2 and removing the angular coordinate θ, we obtain:
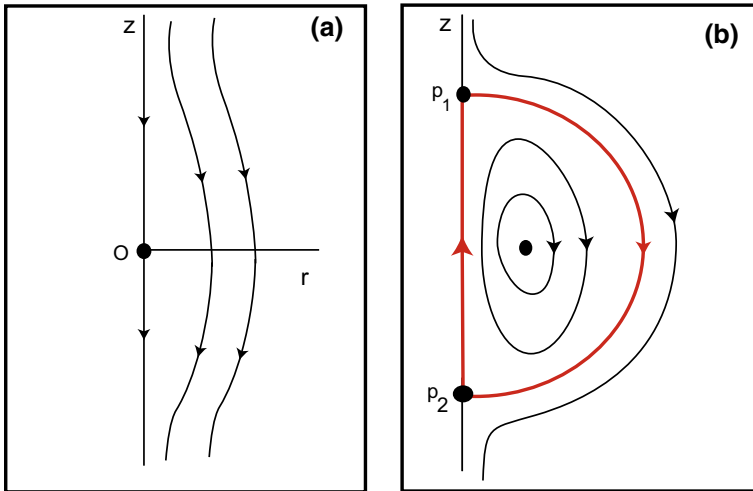
$$\begin{cases} \dot{r} = a_1 rz \\ \dot{z} = b_1 r^2 + b_2 z^2. \end{cases} \tag{10.3}$$

Setting $r^{new} = -\sqrt{|b_1 b_2|}\, r$, $z^{new} = -b_2 z$, and dropping the superscripts "new", we get the differential equation:

$$\begin{cases} \dot{r} = arz \\ \dot{z} = br^2 - z^2 \end{cases} \tag{10.4}$$

where $a = -a_1/b_2$ and $b = \pm 1$. The phase diagram of (10.4) for $a > 0$ and $b = -1$ is shown in Fig. 12a.

---

[5] The author is grateful to one of the reviewers for pointing out this remark.

Fig. 12 **a** Phase diagram of (10.4) for $a > 0$ and $b = -1$. **b** Stable heteroclinic cycle associated to O_1 and O_2 for the differential equation (10.5) with $\mu_1 = 0$

Takens [49] proved that there are six topological types for the normal form (10.4), but from now on, we are only interested in the one characterized by the conditions $b = -1$ and $a > 0$ (Type I of [11]; Case III of [25]). The line defined by $r = 0$ (z-axis) is flow-invariant. According to [25], any generic unfolding of (10.4), truncated at second order, may be written as:

$$\begin{cases} \dot{r} = \mu_1 r + arz \\ \dot{z} = \mu_2 - r^2 - z^2 \end{cases} \tag{10.5}$$

whose flow satisfy the following properties (for $\mu_2 \geq 0$ and $\mu_2 > \frac{\mu_1^2}{a^2}$):

- there are two equilibria of saddle-type, say $p_1 = (0, \sqrt{\mu_2})$, $p_2 = (0, -\sqrt{\mu_2})$, whose eigenvalues of $df^\star$ at the equilibria are $\mu_1 \pm a\sqrt{\mu_2}$ and $\mp 2\sqrt{\mu_2}$;
- there is another equilibrium given by $\left(\sqrt{\mu_2 - \frac{\mu_1^2}{a^2}}, -\frac{\mu_1}{a} \right)$ which is a center;
- for $\mu_1 = 0$, there is a heteroclinic cycle associated to p_1 and p_2;
- for $\mu_1 = 0$, if $G(r, z) = \frac{a}{2} r^{\frac{2}{a}} \left(\mu_2 - \frac{r^2}{1+a} - z^2 \right)$ then the Lie derivative of G with respect to the vector field associated to (10.5) satisfies the equality:

$$\mathcal{L}_v G \equiv 0,$$

meaning that there is a family of non-trivial periodic solutions limiting the inner part of the planar heteroclinic cycle associated to p_1 and p_2. This cycle is Lyapunov stable—see Fig. 12b.

The truncated normal form of order 2 is not enough to our purposes because the heteroclinic cycle is not asymptotically stable.
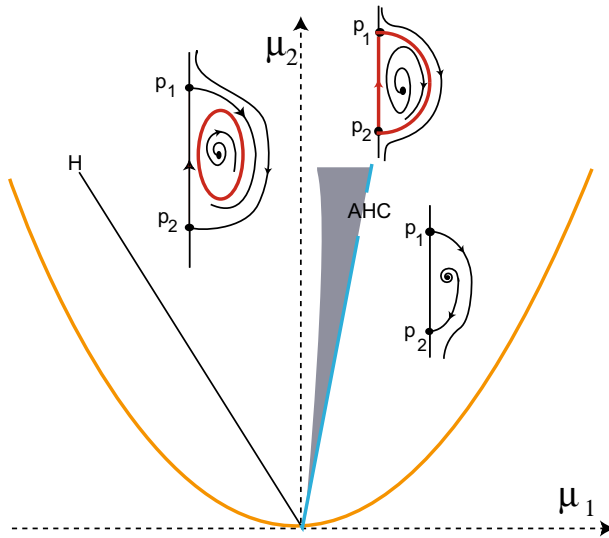
Fig. 13 Bifurcation diagram for the differential equation (10.8) when $3c + e > d + 3f$ and $3(3c + e) + d + 3f < 0$. (H): Hopf bifurcation; (AHC): attracting heteroclinic cycle. The grey region is the wedge shaped region $\mathcal{W}$ where Proposition 10.1 is valid

10.2 Truncating at Order 3

Truncating at third order any generic unfolding of (10.4) with $a > 0$ and $b = -1$, we obtain:

$$\begin{cases} \dot{r} = \mu_1 r + arz + cr^3 + drz^2 \\ \dot{z} = \mu_2 - r^2 - z^2 + er^2z + fz^3. \end{cases} \tag{10.6}$$

Assuming that the new parameters $c, d, e, f \in \mathbb{R}$ satisfy the open conditions:

$$3c + e > d + 3f \quad \text{and} \quad 3(3c + e) + d + 3f < 0, \tag{10.7}$$

the flow of (10.6) exhibits a heteroclinic cycle associated to

$$\tilde{p}_1 \approx (0, \sqrt{\mu_2} + f/2) \quad \text{and} \quad \tilde{p}_2 \approx (0, -\sqrt{\mu_2} + f/2)$$

at all points (μ_1, μ_2) lying at the line AHC defined by

$$AHC: \quad \mu_2 = \frac{-4\mu_1}{3(3c + e) + d + 3f} + O(\sqrt{\mu_2}).$$

This cycle has a non-empty basin of attraction [25,31]. Line AHC is depicted in Fig. 13.

10.3 General Perturbations

Adding the angular coordinate θ to Eq. (10.6), we define a $\mathbb{SO}(2)$-equivariant vector field, say $f_{(\mu_1, \mu_2)}$. Its flow has cycle associated to the lift of $\tilde{p}_1$ and $\tilde{p}_2$, say O_1 and O_2 with non-empty basin of attraction. This cycle is made by one 1D and one 2D heteroclinic connections associated to two hyperbolic saddles-foci with different Morse indices. The coincidence of

the invariant manifolds of the hyperbolic saddle-foci is exceptional and they are expected to split.

Generic analytic unfoldings of the Hopf-zero singularities were considered in [21]; the authors introduced an extra parameter $\varepsilon = \sqrt{\mu_2}$ and obtained a singular perturbation problem with a pure rotation when $\varepsilon = 0$ or a family with rotation speed tending to $+\infty$ as $\varepsilon \to 0$. Since the imaginary part of the eigenvalues of the vector field at the equilibria has the form $O(1/\varepsilon)$, this means that $K_\omega \to 0$; details in Section 3 of [21]. In the present work, we are interested in particular unfoldings of a Hopf-zero singularity.

Definition 3 A *Gaspard-type unfolding* of a Hopf-zero singularity $f^\star$ (with $a > 0$ and $b = -1$ in (10.4)) has the form:

$$\begin{cases} \dot{r} = \mu_1 r + arz + cr^3 + drz^2 + O(\varepsilon)\mathcal{H}_1(r,z) \\ \dot{\theta} = 1 + O(\varepsilon)\mathcal{H}_2(r,z) \\ \dot{z} = \mu_2 - r^2 - z^2 + er^2 z + fz^3 + O(\varepsilon)\mathcal{H}_3(r,z) \end{cases}, \qquad (10.8)$$

where $\mathcal{H}_1, \mathcal{H}_2, \mathcal{H}_3$ are arbitrary smooth functions of degree greater than three in the variables r and z (*i.e.* they have the form of equations (2.15) and (2.16) of Gaspard [22]).

Proposition 10.1 *Let $f^\star$ be a Hopf-zero singularity (with $a > 0$ and $b = -1$ in (10.4)). Then there exists an analytic curve $\mathcal{S}$ in the parameter space (μ_1, μ_2) and a domain $\mathcal{W}$ contained in a wedge shaped neighborhood of $\mathcal{S}$ such that: if $(\mu_1, \mu_2) \in \mathcal{W}$ then any Gaspard-type unfolding of $f^\star$ contains strange attractors (of Hénon-type) with an ergodic SRB measure.*

In the following proof, Hypothesis **(P8)** is implicit; it corresponds to the expected unfolding from the coincidence of the two-dimensional invariant manifolds of the equilibria; see Remark 5.1.

Proof We apply Theorem E to prove Proposition 10.1. Indeed, if $(\mu_1, \mu_2) \in AHC =: \mathcal{S}$, then the flow of $f_{(\mu_1, \mu_2)}$ satisfies:

- there are two hyperbolic saddle-foci O_1 and O_2 satisfying **(P1)–(P2)**;
- the manifolds $W^u(O_2)$ and $W^s(O_1)$ coincide and one branch of $W^u(O_1)$ coincide with $W^s(O_2)$—see Remark 9.4. In particular, there is a heteroclinic cycle associated to O_1 and O_2 with non-empty basin of attraction, meaning that **(P3)–(P4a)** are satisfied;
- by construction on the way the angular coordinate is acting on (10.6), the saddle-foci have the same chirality—**(P5)** is valid;
- by hypothesis, we perturb $f_{(\mu_1, \mu_2)}$ in such a way that the manifolds $W^u(O_2)$ and $W^s(O_1)$ do not intersect and the one-dimensional manifolds are preserved, emerging an attracting 2-torus. The dynamics on it exhibits intervals of frequency locking and irrational flow as the rotation number varies. This perturbation correspond to **(P6)–(P7)**.

Adding the $O(\varepsilon)$-terms will correspond to generic perturbations (without symmetry) that break the attracting two-dimensional torus [25]. Observe that $\lim_{\varepsilon \to 0} K_\omega = +\infty$ since the imaginary part of the eigenvalues of the vector field at the equilibria has the form $O(1/\varepsilon)$ (cf. pp. 4444 of [21]). By Theorem E, the result follows, where the parameter ε plays the role of λ.   □

Remark 10.2 Besides the break of the two-dimensional attracting torus, adding generic $O(\varepsilon)$-terms to $f_{(\mu_1, \mu_2)}$ may imply that the 1D-connection is also broken. This does not affect the proof of Proposition 10.1 since the existence of strange attractors has been obtained *via Torus-breakdown phenomena*, which occur even when the 1D-connection is broken.

Theorem E cannot be applied directly for generic unfoldings of the Hopf-zero singularity because there is no chance to express a generic Hopf-zero singularities as perturbations of a vector field whose flow has an attracting heteroclinic cycle.

10.4 Discussion and Conjecture

Following Bonckaert and Fontich [14], when the scaling parameters defined in [21] tend to 0, the invariant manifolds have a limit position given by the invariant manifolds of the equilibria at the 2-jet of the singularity when $z > 0$. Therefore, for any generic unfolding of the Hopf-zero singularity (Type I of [11]), the splitting distance is well defined for the $1D$ and $2D$-connections. The first case was obtained in [9]—the distance $\mathcal{S}^1$ between the 1D invariant manifolds is exponentially small with respect to $\varepsilon > 0$ and the coefficient in front of the dominant term depends on the full jet of the singularity. The splitting function for the 2D invariant manifolds, say $\mathcal{S}^2$, has been obtained in [10].

When the manifolds $W^u(O_2)$ and $W^s(O_1)$ intersect transversely, conclusive results are given in [11]: any generic analytic unfolding of a Hopf-zero singularity exhibits Shilnikov bifurcations and strange attractors [16,28].

When the two-dimensional manifolds of the saddle-foci do not intersect (see [10] and case $\sigma \gg O(\varepsilon)$ of [11][6]), there exist trapping regions which prevent the existence of Shilnikov homoclinic cycles. In particular, the route *Shilnikov bifurcations $\Rightarrow$ Strange attractors* is not possible. With that configuration (the invariant manifolds of the saddle-foci do not intersect), the existence of suspended horseshoes may be ensured by our Theorem D provided its hypotheses are satisfied—see Remark 9.4. Distances $\mathcal{S}^1$ ([9]) and $\mathcal{S}^2$ ([10]) have to be introduced in the definition of the transition maps. We conjecture that generic analytic unfoldings of a Hopf-zero singularity also include strange attractors created by the Torus-breakdown mechanism. We defer this task for a future work.

A Glossary

For $\varepsilon > 0$ small, consider the two-parameter family of C^3-smooth autonomous differential equations

$$\dot{x} = f_{(A,\lambda)}(x) \qquad x \in \mathbb{S}^3 \qquad A, \lambda \in [0, \varepsilon] \tag{A.1}$$

Denote by $\varphi_{(A,\lambda)}(t, x)$, $t \in \mathbb{R}$, the associated flow.

A.1 Symmetry

Given a group $\mathcal{G}$ of endomorphisms of $\mathbb{S}^3$, we will consider two-parameter families of vector fields $(f_{(A,\lambda)})$ under the equivariance assumption $f_{(A,\lambda)}(\gamma x) = \gamma f_{(A,\lambda)}(x)$ for all $x \in \mathbb{S}^3$, $\gamma \in \mathcal{G}$ and $(A, \lambda) \in [0, \varepsilon]^2$. For an isotropy subgroup $\widetilde{\mathcal{G}} < \mathcal{G}$, we will write $\mathrm{Fix}(\widetilde{\mathcal{G}})$ for the

---

[6] The condition $\sigma \gg O(\varepsilon)$ does not refer to a class of unfoldings, but to a region in the parameter space associated to the unfolding.

vector subspace of points that are fixed by the elements of $\widetilde{\mathcal{G}}$. Observe that, for $\mathcal{G}-$equivariant differential equations, the subspace $\mathrm{Fix}(\widetilde{\mathcal{G}})$ is flow-invariant.

A.2 Attracting Set

A subset Ω of a topological space $\mathcal{M}$ for which there exists a neighborhood $U \subset \mathcal{M}$ satisfying $\varphi(t, U) \subset U$ for all $t \geq 0$ and $\bigcap_{t \in \mathbb{R}^+} \varphi(t, U) = \Omega$ is called an *attracting set* by the flow φ, not necessarily connected. Its basin of attraction, denoted by $\mathbf{B}(\Omega)$ is the set of points in $\mathcal{M}$ whose orbits have $\omega-$limit in Ω. We say that Ω is *asymptotically stable* (or that Ω is a *global attractor*) if $\mathbf{B}(\Omega) = \mathcal{M}$. An attracting set is said to be *quasi-stochastic* if it encloses periodic solutions with different Morse indices, structurally unstable cycles, sinks and saddle-type invariant sets.

A.3 Heteroclinic Structures

Suppose that O_1 and O_2 are two hyperbolic saddle-foci of $f_{(A,\lambda)}$ with different Morse indices (dimension of the unstable manifold). There is a *heteroclinic cycle* associated to O_1 and O_2 if $W^u(O_1) \cap W^s(O_2) \neq \emptyset$ and $W^u(O_2) \cap W^s(O_1) \neq \emptyset$. For $i, j \in \{1, 2\}$, the non-empty intersection of $W^u(O_i)$ with $W^s(O_j)$ is called a *heteroclinic connection* between O_i and O_j, and will be denoted by $[O_i \rightarrow O_j]$. Although heteroclinic cycles involving equilibria are not a generic feature within differential equations, they may be structurally stable within families of systems which are equivariant under the action of a compact Lie group $\mathcal{G} \subset \mathbb{O}(n)$, due to the existence of flow-invariant subspaces [25].

A.4 Bykov Cycle

A heteroclinic cycle between two hyperbolic saddle-foci of different Morse indices, where one of the connections is transverse (and so stable under small perturbations) while the other is structurally unstable, is called a Bykov cycle. A *Bykov network* is a connected union of heteroclinic cycles, not necessarily in finite number. We refer to [29] for an overview of heteroclinic bifurcations and substantial information on the dynamics near different kinds of heteroclinic cycles and networks.

A.5 Suspended Horseshoe

Given $(A, \lambda) \in [0, \varepsilon]^2$, suppose that there is a cross-section $\mathcal{S}_\lambda$ to the flow $\varphi_{(A,\lambda)}$ such that $\mathcal{S}_{(A,\lambda)}$ contains a compact set $\mathcal{K}_{(A,\lambda)}$ invariant by the first return map $\mathcal{F}_{(A,\lambda)}$ to $\mathcal{S}_{(A,\lambda)}$. Assume also that $\mathcal{F}_{(A,\lambda)}$ restricted to $\mathcal{K}_{(A,\lambda)}$ is conjugate to a full shift on a finite alphabet. Then the *suspended horseshoe associated to $\mathcal{K}_{(A,\lambda)}$* is the flow-invariant set $\widetilde{\mathcal{K}_{(A,\lambda)}} = \{\varphi_\lambda(t, x) : t \in \mathbb{R}, \ x \in \mathcal{K}_{(A,\lambda)}\}$.

A.6 SRB Measure

Given an attracting set Ω for a continuous map $R : \mathcal{M} \rightarrow \mathcal{M}$ of a compact manifold $\mathcal{M}$, consider the Birkhoff average with respect to the continuous function $T : \mathcal{M} \rightarrow \mathbb{R}$ on the

R-orbit starting at $x \in \mathcal{M}$:

$$L(T, x) = \lim_{n \in \mathbb{N}} \quad \frac{1}{n} \sum_{i=0}^{n-1} T \circ R^i(x). \tag{A.2}$$

Suppose that, for Lebesgue almost all points $x \in \mathbf{B}(\Omega)$, the limit (A.2) exists and is independent on x. Then L is a continuous linear functional in the set of continuous maps from $\mathcal{M}$ to $\mathbb{R}$ (denoted by $C(\mathcal{M}, \mathbb{R})$). By the Riesz Representation Theorem, it defines a unique probability measure μ such that:

$$\lim_{n \in \mathbb{N}} \quad \frac{1}{n} \sum_{i=0}^{n-1} T \circ R^i(x) = \int_{\Omega} T \, d\mu \tag{A.3}$$

for all $T \in C(\mathcal{M}, \mathbb{R})$ and for Lebesgue almost all points $x \in \mathbf{B}(\Omega)$. If there exists an ergodic measure μ supported in Ω such that (A.3) is satisfied for all continuous maps $T \in C(\mathcal{M}, \mathbb{R})$ for Lebesgue almost all points $x \in \mathbf{B}(\Omega)$, where $\mathbf{B}(\Omega)$ has positive Lebesgue measure, then μ is called a SRB measure and Ω is a SRB attractor.

References

1. Afraimovich, V.S., Shilnikov, L.P.: On invariant two-dimensional tori, their breakdown and stochasticity. In: Methods of the Qualitative Theory of Differential Equations, Gor'kov. Gos. University, pp. 3–26 (1983). Translated in: Amer. Math. Soc. Transl., (2), vol. 149 (1991) 201–212
2. Afraimovich, V.S., Bykov, V.V., Shilnikov, L.P.: On the structurally unstable attracting limit sets of Lorenz attractor type. Tran. Moscow Math. Soc. **2**, 153–215 (1982)
3. Afraimovich, V.S., Hsu, S.-B., Lin, H.E.: Chaotic behavior of three competing species of May–Leonard model under small periodic perturbations. Int. J. Bifurc. Chaos **11**(2), 435–447 (2001)
4. Afraimovich, V.S., Hsu, S.B.: Lectures on Chaotic Dynamical Systems. American Mathematical Society and International Press, Boston (2002)
5. Aguiar, M.: Vector Fields with Heteroclinic Networks. Ph.D. thesis, Departamento de Matemática Aplicada, Faculdade de Ciências da Universidade do Porto (2003)
6. Aguiar, M.A.D., Castro, S.B.S.D., Labouriau, I.S.: Dynamics near a heteroclinic network. Nonlinearity **18**, 391–414 (2005)
7. Anishchenko, V., Safonova, M., Chua, L.: Confirmation of the Afraimovich–Shilnikov torus-breakdown theorem via a torus circuit. IEEE Trans. Circuits Syst. I Fundam. Theory Appl. **40**(11), 792–800 (1993)
8. Aronson, D., Chory, M., Hall, G., McGehee, R.: Bifurcations from an invariant circle for two-parameter families of maps of the plane: a computer-assisted study. Commun. Math. Phys. **83**(3), 303–354 (1982)
9. Baldomá, I., Castejón, O., Seara, T.M.: Exponentially small heteroclinic breakdown in the generic Hopf-Zero singularity. J. Dyn. Differ. Equ. **25**(2), 335–392 (2013)
10. Baldomá, I., Castejón, O., Seara, T.M.: Breakdown of a 2D heteroclinic connection in the Hopf-zero singularity (II). The generic case. J. Nonlinear Sci. **28**(4), 1489–1549 (2018)
11. Baldomá, I., Ibáñez, S., Seara, T.: Hopf-Zero singularities truly unfold chaos. Commun. Nonlinear Sci. Numer. Simul. **84**, 105162 (2020)
12. Benedicks, M., Carleson, L.: The dynamics of the Hénon map. Ann. Math. **133**(1), 73–169 (1991)
13. Bessa, M., Rodrigues, A.A.P.: Dynamics of conservative Bykov cycles: tangencies, generalized Cocoon bifurcations and elliptic solutions. J. Differ. Equ. **261**(2), 1176–1202 (2016)
14. Bonckaert, P., Fontich, E.: Invariant manifolds of dynamical systems close to a rotation: transverse to the rotation axis. J. Differ. Equ. **214**(1), 128–155 (2005)
15. Boyland, P.L.: Bifurcations of circle maps: Arnold tongues, bistability and rotation intervals. Commun. Math. Phys. **106**, 353–381 (1986)
16. Broer, H., Vegter, G.: Subordinate Shilnikov bifurcations near some singularities of vector fields having low codimension. Ergodic Theory Dyn. Syst. **4**, 509–525 (1984)
17. Bykov, V.V.: Orbit structure in a neighborhood of a separatrix cycle containing two saddle-foci. Am. Math. Soc. Transl. **200**, 87–97 (2000)

18. Carvalho, M., Rodrigues, A.A.P.: Complete set of invariants for a Bykov attractor. Regul. Chaotic Dyn. **23**, 227–247 (2018)
19. Colli, E.: Infinitely many coexisting strange attractors. Ann. Inst. H. Poincaré **15**, 539–579 (1998)
20. Deng, B.: The Shilnikov problem, exponential expansion, strong λ-Lemma, C^1 linearisation and homoclinic bifurcation. J. Differ. Equ. **79**, 189–231 (1989)
21. Dumortier, F., Ibáñez, S., Kokubu, H., Simó, C.: About the unfolding of a Hopf-zero singularity. Discrete Contin. Dyn. Syst. **33**(10), 4435–4471 (2013)
22. Gaspard, P.: Local birth of homoclinic chaos. Physica D **62**(1–4), 94–122 (1993)
23. Gavrilov, N.K., Shilnikov, L.P.: On three-dimensional dynamical systems close to systems with a structurally unstable homoclinic curve. Part I: Math. USSR Sbornik **17**, 467–485 (1972). Part II: ibid **19**, 139–156 (1973)
24. Gonchenko, S.V., Shilnikov, L.P., Turaev, D.V.: Quasiattractors and homoclinic tangencies. Comput. Math. Appl. **34**(2–4), 195–227 (1997)
25. Guckenheimer, J., Holmes, P.: Nonlinear Oscillations, Dynamical Systems, and Bifurcations of Vector Fields. Applied Mathematical Sciences, vol. 42. Springer, Berlin (1983)
26. Herman, M.: Mesure de Lebesgue et Nombre de Rotation. Lecture Notes in Mathematics, vol. 597, pp. 271–293. Springer, Berlin (1977)
27. Hirsch, M.W., Pugh, C., Shub, M.: Invariant manifolds. Bull. Am. Math. Soc. **76**(5), 1015–1019 (1970)
28. Homburg, A.J.: Periodic attractors, strange attractors and hyperbolic dynamics near homoclinic orbits to saddle-focus equilibria. Nonlinearity **15**, 1029–1050 (2002)
29. Homburg, A.J., Sandstede, B.: Homoclinic and Heteroclinic Bifurcations in Vector Fields. Handbook of Dynamical Systems, vol. 3, pp. 379–524. North Holland, Amsterdam (2010)
30. Knobloch, J., Lamb, J.S.W., Webster, K.N.: Using Lin's method to solve Bykov's problems. J. Differ. Equ. **257**(8), 2984–3047 (2014)
31. Kuznetsov, Y.A.: Elements of Applied Bifurcation Theory. Applied Mathematical Sciences, vol. 112, 3rd edn. Springer, New York (2004)
32. Koon, W.S., Lo, M., Marsden, J., Ross, S.: Heteroclinic Connections Between Periodic Orbits and Resonance Transition in Celestial Mechanics. Control and Dynamical Systems Seminar, California Institute of Technology, Pasadena, California (1999)
33. Labouriau, I.S., Rodrigues, A.A.P.: Global generic dynamics close to symmetry. J. Differ. Equ. **253**(8), 2527–2557 (2012)
34. Labouriau, I.S., Rodrigues, A.A.P.: Dense heteroclinic tangencies near a Bykov cycle. J. Differ. Equ. **259**(12), 5875–5902 (2015)
35. Labouriau, I.S., Rodrigues, A.A.P.: Global bifurcations close to symmetry. J. Math. Anal. Appl. **444**(1), 648–671 (2016)
36. Lamb, J.S.W., Teixeira, M.A., Webster, K.N.: Heteroclinic bifurcations near Hopf-zero bifurcation in reversible vector fields in $\mathbb{R}^3$. J. Differ. Equ. **219**, 78–115 (2005)
37. Mora, L., Viana, M.: Abundance of strange attractors. Acta Math. **171**(1), 1–71 (1993)
38. Newhouse, S.E.: Diffeomorphisms with infinitely many sinks. Topology **13**, 9–18 (1974)
39. Newhouse, S.E.: The abundance of wild hyperbolic sets and non-smooth stable sets for diffeomorphisms. Publ. Math. Inst. Hautes Études Sci. **50**, 101–151 (1979)
40. Ovsyannikov, I.M., Shilnikov, L.P.: On systems with a saddle-focus homoclinic curve. Math. USSR Sb. **58**, 557–574 (1987)
41. Palis, J., Takens, F.: Hyperbolicity and Sensitive Chaotic Dynamics at Homoclinic Bifurcations: Fractal Dimensions and Infinitely Many Attractors in Dynamics. Cambridge University Press, Cambridge (1995)
42. Passeggi, A., Potrie, R., Sambarino, M.: Rotation intervals and entropy on attracting annular continua. Geom. Topol. **22**(4), 2145–2186 (2018)
43. Rodrigues, A.A.P.: Persistent switching near a heteroclinic model for the geodynamo problem. Chaos Solitons Fractals **47**, 73–86 (2013)
44. Rodrigues, A.A.P.: Repelling dynamics near a Bykov cycle. J. Dyn. Differ. Equ. **25**(3), 605–625 (2013)
45. Rodrigues, A.A.P., Labouriau, I.S.: Spiralling dynamics near heteroclinic networks. Physica D **268**, 34–49 (2014)
46. Rodrigues, A.A.P., Labouriau, I.S., Aguiar, M.A.D.: Chaotic double cycling. Dyn. Sys. Int. J. **26**(2), 199–233 (2011)
47. Shilnikov, L.P.: A contribution to the problem of the structure of an extended neighborhood of a rough equilibrium state of saddle-focus type. Math. USSR Sb. **10**, 91–102 (1970)
48. Shilnikov, A., Shilnikov, L.P., Turaev, D.: On some mathematical topics in classical synchronization. A tutorial. Int. J. Bifurc. Chaos. Appl. Sci. Eng. **14**, 2143–2160 (2004)
49. Takens, F.: Singularities of vector fields. Publ. Math. l'IHES **43**(1), 47–100 (1974)

50. Wang, Q., Oksasoglu, A.: Dynamics of homoclinic tangles in periodically perturbed second-order equations. J. Differ. Equ. **250**(2), 710–751 (2011)
51. Wang, Q., Young, L.S.: From invariant curves to strange attractors. Commun. Math. Phys. **225**, 275 (2002)
52. Wiggins, S.: Global Bifurcations and Chaos. Analytical Methods. Applied Mathematical Sciences, vol. 73. Springer, New York (1988)
53. Yorke, J.A., Alligood, K.T.: Cascades of period-doubling bifurcations: a prerequisite for horseshoes. Bull. Am. Math. Soc. (N.S.) **9**(3), 319–322 (1983)

Publisher's Note Springer Nature remains neutral with regard to jurisdictional claims in published maps and institutional affiliations.